Journal of Visualized Experiments

Real-Time Proxy-Control of Re-Parameterized Peripheral Signals Using a Close-Loop Interface

--Manuscript Draft--

Article Type:	Methods Article - Author Produced Video
Manuscript Number:	JoVE61943R2
Full Title:	Real-Time Proxy-Control of Re-Parameterized Peripheral Signals Using a Close-Loop Interface
Corresponding Author:	Vilelmini Kalampratsidou Rutgers University Piscataway Township, New Jersey UNITED STATES
Corresponding Author's Institution:	Rutgers University
Corresponding Author E-Mail:	vilelmini.kalabratsidou@gmail.com
Order of Authors:	Vilelmini Kalampratsidou
	Steven Kemper
Additional Information:	
Question	**Response**
Please specify the section of the submitted manuscript.	Behavior
Please indicate whether this article will be Standard Access or Open Access.	Standard Access (US$1200)
Please confirm that you have read and agree to the terms and conditions of the author license agreement that applies below:	I agree to the Author License Agreement
Please provide any comments to the journal here.	

TITLE

Real-Time Proxy-Control of Re-Parameterized Peripheral Signals Using a Close-Loop Interface

AUTHORS AND AFFILIATIONS

Vilelmini Kalampratsidou[1, 2], Steven Kemper[3]

[1]Center for Cognitive Science, Rutgers University, New Brunswick, NJ, USA
[2]Department of Computer Science, Rutgers University, New Brunswick, NJ, USA
[3]Music Department, Mason Gross School of the Arts, Rutgers University, New Brunswick, NJ, USA

Corresponding Author:
Vilelmini Kalampratsidou, vilelmini.kalabratsidou@gmail.com

Email Addresses of Authors:
Steven Kemper, skemper@mgsa.rutgers.edu

KEYWORDS

close-loop interface, co-adaptive interface, interactive interface, sensory augmentation, sensory substitution, auditory feedback, bodily signal sonification, heartrate, kinematics, stochastic analyses, forward kinematic map, kinematic chain, avatar.

SUMMARY

We present protocols and methods of analyses to build co-adaptive interfaces that stream, parameterize, analyze, and modify human body and heart signals in close-loop. This setup interfaces signals derived from the peripheral and central nervous systems of the person with external sensory inputs to help track biophysical change.

ABSTRACT

The fields that develop methods for sensory substitution and sensory augmentation have aimed to control external goals using signals from the central nervous systems (CNS). Less frequent however, are protocols that update external signals self-generated by interactive bodies in motion. There is a paucity of methods that combine the body-heart-brain biorhythms of one moving agent to steer those of another moving agent during dyadic exchange. Part of the challenge to accomplish such a feat has been the complexity of the setup using multimodal biosignals with different physical units, disparate time scales and variable sampling frequencies.

In recent years, the advent of wearable bio sensors that can non-invasively harness multiple signals in tandem, has opened the possibility to re-parameterize and update the peripheral signals of interacting dyads, in addition to improving brain- and/or body-machine interfaces. Here we present a co-adaptive interface that updates efferent somatic-motor output (including kinematics and heart rate) using biosensors; parameterizes the stochastic biosignals, sonifies this output, and feeds it back in re-parameterized form as visuo/audio-kinesthetic reafferent input. We illustrate the methods using two types of interactions, one involving two humans and another involving a human and its avatar interacting in near real time. We discuss the new methods in

the context of possible new ways to measure the influences of external input on internal somatic-sensory-motor control.

INTRODUCTION

The Natural Close-Loop Controller

Sensory-motor information flows continuously between the brain and the body to produce well-organized, coordinated behaviors. Such behaviors can be studied while focusing on the person's actions alone, as in a monologue style (**Figure 1A**), or during complex dynamic actions shared between two agents in a dyad, as in a dialogue style (**Figure 1B**). Yet, a third option is to assess such complex interactions through a proxy controller, within the context of a human-computer closed loop interface (**Figure 1C**). Such interface can track the moment-by-moment movements' fluctuations contributed by each agent in the dyad, and by the type of cohesiveness that self-emerges from their synchronous interactions, helping steer the dyad's rhythms in desirable ways.

[Figure 1 here]

The overall goal of this method is to show that it is possible to harness, parameterize and re-parameterize the moment-by-moment fluctuations in biorhythmic activities of bodies in motion, as two agents engage in dyadic exchange that may involve two humans, or a human and his/her self-moving avatar.

Investigations on how the brain may control actions and predict their sensory consequences have generated many lines of theoretical enquiries in the past[1-3] and produced various models of neuromotor control[4-8]. One line of research in this multi-disciplinary field has involved the development of close-loop brain-machine or brain-computer interfaces. These types of setups offer ways to harness and adapt the CNS signals to control an external device, such as a robotic arm[9-11], an exoskeleton[12], a cursor on a computer screen[13] (among others). All these external devices share the property that they do not have own intelligence. Instead, the brain trying to control them does have, and part of the problem that the brain faces is to learn how to predict the consequences of the motions that it generates in these devices (e.g., the cursor's motions, the robotic arm's motions, etc.) while generating other supportive motions that contribute to the overall sensory motor feedback in the form of kinesthetic reafference. Often, the overarching aim of these interfaces has been to help the person behind that brain bypass an injury or disorder, to regain the transformation of his/her intentional thoughts into volitionally controlled physical acts of the external device. Less common however has been the development of interfaces that attempt to steer the movements of bodies in motion.

Much of the original research on brain-machine interfaces focus on the control of the central nervous system (CNS) over body parts that can accomplish goal-directed actions[9,14-17]. There are, however, other situations whereby using the signals derived from activities of the peripheral nervous systems (PNS), including those of the autonomic nervous systems (ANS), is informative enough to influence and steer the signals of external agents, inclusive of another human or avatar, or even interacting humans (as in **Figure 1C**). Unlike with a robotic arm or cursor, the other agent in this case, has intelligence driven by a brain (in the case of the avatar that has been

endowed with the person's motions, or of another agent, in the case of an interacting human dyad).

A setup that creates an environment of a co-adaptive close-loop interface with dyadic exchange may be of use to intervene in disorders of the nervous systems whereby the brain cannot volitionally control one's own body in motion at will, despite not having physically severed the bridge between the CNS and the PNS. This may be the case owing to noisy peripheral signals whereby the feedback loops to aid the brain continuously monitor and adjust its own self-generated biorhythms may have been disrupted. This scenario arises in patients with Parkinson's disease[18,19], or in participants with autism spectrum disorders with excess noise in their motor output. Indeed, in both cases, we have quantified high levels of noise-to-signal ratio in the returning kinesthetic signals derived from the speed of their intended movements[20-22] and from the heart[23]. In such cases, trying to master the brain-control of external signals, while also trying to control the body in motion, may result in a self-reactive signal from the re-entrant (re-afferent) stream of information that the brain receives from the continuous (efferent) motor stream at the periphery. Indeed, the moment-by-moment fluctuations present in such self-generated efferent motor stream contain important information useful to aid the prediction of the sensory consequences of purposeful actions[24]. When this feedback is corrupted by noise, it becomes difficult to predictably update the control signals and bridge intentional plans with physical acts.

If we were to extend such feedback loop to another agent and control the person and agent's interactions through a third party (**Figure 1C**), we may have a chance to steer each other's performances in near real time. This would provide us with the proof of concept that we would need to extend the notion of co-adaptive brain-body or brain-machine interfaces to treat disorders of the nervous systems that result in poor realization of physical volition from mental intent.

Purposeful actions have consequences, which are precisely characterized by motor stochastic signatures that are context-dependent and enable inference of levels of mental intent with high certainty[25,26]. Thus, an advantage of a new method that leverages dyadic exchange over prior person-centered approaches to the brain machine or brain computer interfaces, is that we can augment the control signals to include the bodily and heart biorhythms that transpire largely beneath the person's awareness, under different levels of intent. In this way, we dampen reactive interference that conscious control tends to evoke in the process of adapting brain-cursor control[17]. We can add more certainty to the predictive process by parameterizing the various signals that we can access. Along those lines, prior work exists using brain and bodily signals in tandem[27-29]; but work involving dyadic interactions captured by brain-bodily signals remains scarce. Further, the extant literature has yet to delineate the distinction between deliberate segments of the action performed under full awareness and transitional motions that spontaneously occur as the consequence of the deliberate ones[30,31]. Here we make that distinction in the context of dyadic exchange, and offer new ways to study this dichotomy[32], while providing examples of choreographed (deliberate) *vs.* improvised (spontaneous) motions in the dance space.

Because of the transduction and transmission delays in the sensory-motor integration and transformation processes[33], it is necessary to have such predictive code in place, to learn to anticipate upcoming sensory input with high certainty. To that end, it is important to be able to characterize the evolution of the noise-to-signal ratio derived from signals in the continuously updating kinesthetic reafferent stream. We then need protocols in place to systematically measure change in motor variability. Variability is inherently present in the moment-by-moment fluctuations of the outgoing efferent motor stream[34]. Since these signals are non-stationary and sensitive to contextual variations[35,36], it is possible to parameterize changes that occur with alterations of the tasks' context. To minimize interference from reactive signals that emerge from conscious CNS control, and to evoke quantifiable changes in the efferent PNS motor stream, we introduce here a proxy close-loop interface that indirectly alters the sensory feedback, by recruiting the peripheral signal that is changing largely beneath the person's self-awareness. We then show ways to systematically measure the change that ensues the sensory manipulations, using stochastic analyses amenable to visualize the process that the proxy close loop interface indirectly evokes in both agents.

Introducing a Proxy Close-Loop Controller

The sensory-motor variability present in the peripheral signals constitute a rich source of information to guide the performance of the nervous systems while learning, adaptation and generalization take place across different contexts[37]. These signals partly emerge as a byproduct of the CNS trying to volitionally control actions but are not the direct goal of the controller. As the person naturally interacts with others, the peripheral signals can be harnessed, standardized and re-parameterized; meaning that their variations can be parameterized and systematically shifted, as one alters the efferent motor stream that continuously re-enters the system as kinesthetic reafference. In such settings, we can visualize the stochastic shifts, capturing with high precision a rich signal that is otherwise lost to the types of grand averaging that more traditional techniques perform.

To achieve the characterization of change under the new statistical platform, we here introduce protocols, standardized data types and analytics that permit the integration of external sensory input (auditory and visual) with internally self-generated motor signals, while the person naturally interacts with another person, or with an avatar version of the person. In this sense, because we are aiming at controlling the peripheral signals (rather than modifying the CNS signals to directly control the external device or media), we coin this a proxy close-loop interface (**Figure 2**). We aim at characterizing the changes in the stochastic signals of the PNS, as they impact those in the CNS.

[Figure 2 here]

The PNS signals can be harnessed non-invasively with wearable sensing technologies that co-register multi-modal efferent streams from different functional layers of the nervous systems, ranging from autonomic to voluntary[32]. We can then measure in near real time the changes in such streams and select those whose changes enhance the signal-to-noise ratio. This efferent motor signal can then be augmented with other forms of sensory guidance (e.g., auditory, visual,

etc.) Because the PNS signals scape full awareness, they are easier to manipulate without much resistance [38]. As such, we use them to help steer the person's performance in ways that may be less stressful to the human system.

Building the Interface

We present the design of the proxy control mediated by a close-loop co-adaptive multimodal interface. This interface steers the real-time multisensory feedback. **Figure 3** displays the general design.

The close-loop interface is characterized by 5 main steps. The 1st step is the **multi-modal data collection** from multiple wearable instruments. The 2nd step is the **synchronization of the multi-modal streams** through the platform of LabStreamingLayer (LSL, https://github.com/sccn/labstreaminglayer) developed by the MoBI group [39]. The 3rd step is the streaming of the LSL data structure to a Python, MATLAB or other programming language interface to **integrate the signals and to empirically parametrize physiological features** (relevant to our experimental setup) **in real-time**. The 4th step is to re-parameterize the selected features extracted from the continuous stream of the bodily signal studied and **augment it using a sensory modality** of choice (e.g., visual, auditory, kinesthetic, etc.) to play it back in the form of sounds or visuals, to augment, substitute or enhance the sensory modality that is problematic in the person's nervous system. Finally, the 5th step is to **re-assess** the stochastic signatures of the signals generated by the system in real time, to select which sensory modality brings the stochastic shifts of the bodily fluctuations to a regime of high certainty (noise minimization) in the prediction of the sensory consequences of the impending action. **This loop is played continuously** throughout the duration of the experiment with the focus on the selected signal, while storing the full performance for subsequent analyses (as depicted in the schematics of **Figure 3** and see[40-47] for an example of *a posteriori* analyses).

[Figure 3 here]

The following sections present the generic protocol of how to build a close-loop interface (as described in **Figure 3**) and describe representative results of two experimental interfaces (elaborately presented in Supplementary Material) involving physical dyadic interaction between two dancers (real close-loop system) and virtual dyadic interaction between a person and an avatar (artificial close-loop system).

PROTOCOL

Study was approved by the Institutional Study Board (IRB) in compliance with the declaration of Helsinki.

1. Participants

1.1. Define the population to be studied and invite them to participate in the study. The present interface can be used in various populations. This protocol and the examples used here

to provide proof of concept are not limited to a specific group.

1.2. Obtain written informed consent of the IRB approved protocol in compliance with the Declaration of Helsinki.

1.3. Ask the participant or guardian to sign the form before the beginning of the experiment.

2. Setup of the Close-Loop Interface

2.1. Setup of kinematic equipment-PNS

2.1.1. Help the participant to carefully wear the LED-based motion-capture costume (body and head, shown in **Figure 3**, step 1 and 5) accompanying the motion-capture system used. The LED markers of the costume will be tracked by the cameras of the system to estimate the location of the moving body in space.

2.1.2. Connect the wireless LED controller (also known as LED driver unit) of the system with the LED cables of the costume by plugging it into the proper port. Turn the device on, and set it on the streaming mode.

2.1.3. Turn on the server of the motion-capture system.

2.1.4. Open a web-browser, visit the server address, and sign-in (sign-in info must be provided by the company upon purchase of the product).

2.1.5. Calibrate the system as needed (for example, calibrate the system if this is the first time to use the equipment, otherwise move to step 2.1.17).

2.1.6. Open the calibration tool of the motion-capture system and select **Calibration Wizard**.

2.1.7. Make sure that the entry of the server number in the text-field on the left-upper side of the interface is correct and click **Continue**.

2.1.8. Connect the wand to the first port of the LED controller and turn ON the controller and click **Continue**. Once the wand is connected, its LED markers will be turned on and will appear on the display, in the camera views.

2.1.9. Place the wand in the center of the camera view-field, confirm that it can be recorded by the cameras, and click **Continue**.

2.1.10. Move the wand throughout the space by keeping it vertical and drawing cylinders. Make sure that the motion is captured by at least 3 cameras every time and is registered on the view field of each camera making it green. Do this for all cameras.

2.1.11. Once the view-field of each camera has been fully registered (it is all green), click **Continue** and wait for calibration computations to be executed.

NOTE: Once calibration is completed, the camera location along with the LED markers will be seen on the display, as they are physically placed in the room. At this point, the user may resume calibration because it is done, or continue aligning the system.

2.1.12. Hold the wand vertically and place the side with the LED closer to the end of the wand on the ground, where the origin of the 3D space must be set (point (0,0,0)).

2.1.13. Hold the wand stable until registered. Once registered, the screen flashes green. A point indicating the origin of the reference frame on the space will appear on the interface and the next alignment axis, x-axis, will be highlighted green.

2.1.14. Move the wand, maintaining the same orientation (vertically), at the point of the x-axis and hold it stable until registered.

2.1.15. Repeat for the z-axis. Once the point of the z-axis is registered, the calibration is complete.

2.1.16. Click **Finish** to exit calibration.

2.1.17. Open the interface of the motion-capture system and click **Connect** to start streaming the data from the LED markers. Once the connection is established, the position of the markers will be displayed on the virtual world of the interface.

2.1.18. Create the virtual skeleton (automatically estimate the bone positions of the body from the position data collected from the LED markers of the costume, as shown **Figure 8 step2**).

2.1.19. Right click on **Skeletons** on the right side of the window and select **New skeleton**.

2.1.20. Choose **Marker Mapping** and then select the proper file (provided by the company based on the interface version that is used). Then, click **OK**.

2.1.21. Ask participant to stay stable on the T-pose (straight up posture with arms open on the sides).

2.1.22. Right click on skeleton and select **Generate skeleton without training**.

2.1.23. If all steps are correctly performed the skeleton will be generated. Ask participant to move and check how accurately the virtual skeleton follows participant’s movements .

2.1.24. To stream the skeleton data to LSL select **Settings** and **Options** from the main menu.

2.1.25. Open **Owl emulator** and click "start" **Live streaming**.

2.2. Setup of EEG equipment – CNS

2.2.1. Help the same participant to wear the EEG head-cap.

2.2.2. Place the gel electrodes (the traditional gel-based electrodes used with the EEG head-cap) on the head-cap and 2 sticky electrodes (electrodes that work like stickers) on the back side of the right ear for the CMS and DRL sensors.

2.2.3. Fill electrodes with high-conductive gel, as needed, to improve conductivity between the sensor and the scalp.

2.2.4. Connect the electrode-cables on the gel-trodes and the two sticky electrodes.

2.2.5. Stick the wireless monitor on the back of the head-cap and plug in the electrode cables.

2.2.6. Turn on the monitor.

2.2.7. Open the interface of the EEG system.

2.2.8. Select **Use Wi-Fi device** and click **Scan for devices**.

2.2.9. Select **NE Wi-Fi** and **Use this device**.

2.2.10. Click on the head icon, select a protocol that allows the recording of all 32 sensors, and click **Load**.

2.2.11. Make sure that the streamed data of each channel are displayed on the interface.

2.3. Setup of ECG equipment- ANS

2.3.1. Follow the exact steps presented in 2.2 but use channel O1 to connect on the heart rate (HR) extension.

2.3.2. Use a sticky electrode to stick the other end of the extension right below the left ribcage.

2.4. Preparation of LSL for synchronized recording and streaming of kinematic data

2.4.1. Run the LSL application for the motion-capture system by double-clicking on the corresponding icon. Locate the application on the following path of the LSL folder, LSL\labstreaminglayer-master\Apps\PhaseSpace.

2.4.2. On the interface, set the proper server address.

2.4.3. Then, select **File** and **Load configuration**.

2.4.4. Select the proper configuration file (it must be provided by the company based on the product version that is used)

2.4.5. Click **Link**. If no mistakes are made, then no error message will be displayed.

2.5. Prepare LSL for synchronized recording and streaming of EEG and ECG data. No extra steps are required for this equipment.

2.6. Setup of LSL

2.6.1. Run LabRecorder application by double clicking on the file located in the LSL\labstreaminglayer-master\Apps\LabRecorder path of the LSL folder.

2.6.2. Click **Update**. If all instructions are correctly executed, all data types of the motion-capture and EEG system will be seen on the panel Record for streams.

2.6.3. Select directory and name for the data on **Storage location** panel.

2.6.4. Click **Start**. The data collection of the motion-capture and EEG system will begin synchronously.

2.6.5. At the end of the recording click **Stop**. If recording was successful, the data will be located on the directory previously selected. Open the files to confirm that they include the recorded information.

2.7. Real-time analyses and monitoring of the human system

2.7.1. Execute the Matlab, Python, or other code that receives, processes, and augments the streamed data. Example codes corresponding to the representative examples described in the following sections can be found here: https://github.com/VilelminiKala/CloseLoopInterfaceJOVE

2.8. Generation of the augmented sensory feedback

2.8.1. Produce the sensory output using the proper device (e.g., speakers, monitor, among others).

3. Experimental procedure

3.1. Follow the experimental procedure that is defined by the setup, if any.

NOTE: The close-loop interfaces are designed to be intuitively explored and learned. Thus, most of the times no instructions are needed.

REPRESENTATIVE RESULTS

There are various interfaces that can be built based on the protocol presented in the previous section and can be applied on different populations for numerous purposes. Some possible variations are described in section "**Variations of the Presented Close-Loop Interface**" of Supplementary Material.

In this section we demonstrate representative results of 2 sample close-loop interfaces that follow the protocol described in the previous section. The setup, the experimental procedure, and the participants of these studies are explained in depth in sections "**Example 1: Audio Close-loop Interface of a Real Dyadic Interaction**" and "**Example 2: Audio-visual Close-loop Interface of an Artificial Dyadic Interaction**" of the Supplementary File.

Results of Audio Close-loop Interface of a Real Dyadic Interaction

In the study of "Audio close-loop interface of a real dyadic interaction" (elaborately presented in section "**Example 1: Audio Close-loop Interface of a Real Dyadic Interaction**" of Supplementary Material), we used a proxy control interface, illustrated in **Figure 4**, which uses the female dancer's heart signal to alter the music danced. In real time, we performed signal processing to extract the time of the heartbeat and streamed this information to the Max system to alter the speed of the performed song. This way, we played the song back, altered by the biophysical signals. This process led to further alterations of the motions and heartbeat signals.

[Figure 4 here]

Two salsa dancers interacted with the interface and performed a well-rehearsed routine staging a choreography and a spontaneously improvised dance. The dancers had to perform the original version of the song once and a version blended the original tempo of the song with the real-time heartbeat stream. We refer to the later version which was performed twice as alteration 1 and 2 of the song.

In the analysis presented below, we used the heart and audio signal recorded. The peaks of the two signals extracted to estimate MMS trains (see section "Micro-movements Spikes" in Supplementary File), which preserve high frequency fluctuations as shown in **Figure 5**.

[Figure 5 here]

The MMS trains were well characterized as a continuous random process, well represented byvthe continuous Gamma family of probability distributions. MLE deemed this continuous family of distributions as the best fit for both data sets (see explanation in section "Gamma Distribution" of **Supplementary Material** and **Supplementary Figure 2**). This type of random process was used to track the shifts in stochastic signatures of the biorhythms self-generated by bio signals from the human nervous systems.

From the empirically estimated shape and scale Gamma parameters, we obtain the Gamma

moments, the mean, the variance, the skewness, and the kurtosis (see details of the analysis in section "Stochastic Analysis" of Supplementary Material). We then plot the estimated PDF. **Figure 6** focuses only on the heart signal and music, but the methods apply similarly to the other biorhythms generated by the kinematics signals presented in [41].

The PDF of the heart and music signal are shown in **Figure 6A-B**, where we highlight the differences between the datasets of the two conditions, deliberate routine and spontaneous improvisation. For each condition, we underscore the shifts in stochastic signatures induced by the temporal alterations of the song. Initially, they dance to the original song. Then, as the heartbeat changes rhythms in real time, the sonified fluctuations in this signal leads the dancers to follow the temporal alterations of the song.

These are denoted alteration 1 and alteration 2. These systematic shifts are described by the Gamma parameters. Then, using the empirically estimated shape and scale parameters, we obtained the four corresponding Gamma moments for the heartbeat and the songs. These are displayed in **Figure 6C** for the heart (top) and the song (bottom) signals.

[Figure 6 here]

The shift of the signatures can be appreciated in these panels (PDF and Gamma moments graphs), thus demonstrating that the methods presented can capture the adaptation of the heart to the alterations of the song that the proxy controller produces in real time. As the songs shift rhythms, so do the heart stochastic signatures and the transition of the stochastic signatures is consistent in direction (which is also a finding in [41] where we studied the shape and scale parameters). Likewise, as the heart's signatures shift, so do the song's signatures. This mirroring effects -the one affects the other and as one shifts consistently towards a direction so does other- follow the close-loop nature of this proxy controller interface. The results underscore the utility of this setup and gives proof of concept that we can systematically shift the person's autonomic biorhythms within the context of dyadic exchange.

Parallel shifts on the stochastic signatures of both the songs and the bodily signals, demonstrate that the co-adaptation of the whole system (participant and interface) is possible using the peripheral signals. This process smoothly transpires beneath the person's awareness and offers proof of concept for the ideas to remotely and systematically shift the person's bio-signals in correspondence with the external sensory feedback of choice. In summary, we can guide the shifting of the stochastic signatures in this continuous random process. The methods enable to capture change and their rate along the stochastic trajectories that we were able to build in near real time.

To ascertain statistical significance in the shifts, we use the non-parametric ANOVA, Kruskal-Wallis test followed by multiple comparisons post hoc test. We compare the signatures of the MMS of the heart data among the six conditions. **Figure 7** shows the multi-comparison of the MMS heart data and corresponding Kruskal-Wallis table. The multi-comparison plot indicates that there is a significant difference between the baseline condition of the original routine dance

(Rout. Or) and the baseline condition of the original improvised dance (Imp. Or). It is also important to notice that the first alterations, Rout. Alt1 and Imp. Alt1, shift to distributions which share comparable means and the same applies to the second alterations, while the variance, skewness and kurtosis shift on the Gamma moments space (**Figure 6C**).

[Figure 7 here]

Results of Audio-Visual Close-Loop Interface of an Artificial Dyadic Interaction

In the study of "Audio-visual close-loop interface of an artificial dyadic interaction" (elaborately presented in section "**Example 2: Audio-visual close-loop Interface of an artificial dyadic interaction**" of **Supplementary Material**), 6 participants interacted with the interface, illustrated in **Figures 8**, which creates their mirrored avatar rendering the person's own movements. The interface embeds position-dependent sounds within the region surrounding the person during the interaction. The participants were naïve as to the purpose of the study. They had to walk around the room and figure out how to control the sound that would surprisingly emerge as they passed by a RoI (regions of interest) that the proxy controller defined.

[Figure 8 here]

Figure 9 demonstrates the results of the audio-visual interface of condition 1 (see **Supplementary File** for more conditions), where the hip location activates the song when the former in located in RoI. This figure shows the PDF and Gamma signatures (see section "Data Types and Analyses" of Supplementary Material) of the hip speed data of 6 different control participants (C1 to C6), when they were inside and outside the RoI volume. The outcomes presented here highlight the personalized differences on the adaptation rate of the individual participants. These are indicated by the shifts of the stochastic signatures, and the individual outcomes emerging inside or outside the RoI volume. For instance, we can notice that the PDF fit to the frequency histograms of the MMS derived from the speed amplitude of the hips of C3 and C4, were more symmetric (higher shape value) and less noisy (lower scale value) when inside the volume. In contrast, the rest of the participants show an opposite pattern.

Empirically, we have found that signatures to the lower-right corner are those of athletes anddancers, performing highly skilled movements. Signatures lie on the upper-left region, comefrom datasets of nervous systems with pathologies, such as those with a diagnosis of autismspectrum disorders ADHD[22,32] and those of a deafferented participant[21]. Within the context of shifting patterns along a stochastic trajectory, we obtain the median values of the shape and scale to define the right lower quadrant (RLQ) and the left upper quadrant (LUQ) where we track the overall quality of the signal to noise ratio by accumulating this information over time. This considers the updating of the median values dynamically defining these quadrants as the person co-adapts its internally generated biorhythms to those externally controlled by the proxy but dependent upon the person's internal ones.

[Figure 9 here]

Table 1 shows p-values obtained from raw (speed) and MMS data comparing the outcome across conditions when the person's body part is inside the VoI *vs*. outside the VoI. The results depicted on the table have been estimated using the non-parametric ANOVA Kruskal-Wallis test.

[Table 1 here]

Figure 1: Different forms of control. (**A**) Self brain-controlled interfaces rely on the close-loop relations between the person's brain and the person's own body, which can self-regulate and self-interact in "monologue" style. This mode attempts the control of self-generated motions, or it may also aim to control external devices. (**B**) "Dialogue" style control is introduced for two dancers that interact with each other and through physical entrainment and turn-taking to attain control over each other's motions. (**C**) "Third party" dialogue control of the dyad is introduced as mediated by a computer interface that harnesses in tandem the bio signals from both dancers, parameterizes it and feeds it back to the dancers in re-parameterized form using audio and/or vision as forms of sensory guidance. The re-parameterization in the examples presented here were attained using audio or visual feedback, enhanced by the real time kinesthetic motor output of one of the dancers to influence the other; or of both dancers, taking turns in some alternating pattern.

Figure 2: **Proxy control of a dyadic interaction using close-loop multi-modal interface**. (**A**) Indirect control of two dancers (dancing salsa) via a computer co-adaptive interface vs. (**B**) an interactive artificial person-avatar dyad controlled by harnessing the peripheral nervous systems signals and re-parameterizing it as sounds and/or as visual input. (**C**) The concept of sonification using a new standardized data type (the micro-movement spikes, MMS) derived from the moment-by-moment fluctuations in biorhythmic signals amplitude/timing converted to vibrations and then to sound. From Physics, we borrow the notions of compressions and rarefactions produced by a tuning fork outputting soundwave as measurable vibrations. Schematics of soundwaves represented as pressure modulated over time in parallel to spike concentrations for sonification. Example of a physical signal to undergo the proposed pipeline from MMS to vibrations and sonification. We use the heart rate signal as input to the interface. This takes fluctuations in the signal's amplitude aligned to the movement onset every 4 seconds of motion and builds MMS trains representing the vibrations. The spike trains from the MMS are standardized from [0,1]. The color of the spikes as per the colorbar, represents the intensity of the signal. We then sonify these vibrations using Max. This sonified signal can be used to play back in A, or to alter in B the interactions with the avatar. Further, in B it is possible to embed the sound in the environment and use the body position to play the sound back at a region of interest (RoI), or to modulate the audio features as a function of distance to the RoI, speed or acceleration of a body part anchored to another body part, when passing by the RoI.

Figure 3: The architecture of the multi-modal peripherally driven close-loop interface concept. Various bodily signals are collected -kinematic data, heart and brain activity (step 1). LSL is used to synchronously co-register and stream the data coming from various equipment to the interface (step 2). Python/MATLAB/C# code is used to continuously parameterize the fluctuations in the signals using a standardized data type and common scale that enables

selecting the source of sensory guidance most adequate to dampen the system's uncertainty (step 3). This real-time enhancement of signal transmission through selected channel(s) then allows re-parameterization of the re-entrant sensory signal to integrate in the continuous motor stream and enhance the lost or corrupted input stream (sensory substitution step 4). Continuous re-assessment closes the loop (step 5) and we save all data for additional future analyses.

Figure 4: The audio based close-loop interface. 1. An ECG-HR wearable device monitors the activity of a salsa dancer during the performance of her routines and feeds the signals to the interface at 500Hz. 2. Our interface analyses the ECG data in real time. In each frame, it filters the raw data, extracts the R peaks of the QRS complex; and streams the peak detection to MAX. 3. A third-party interface blends the speed of the audio with the speed of the heartrate. 4. The altered song is played back to the dancers.

Figure 5: Estimation of MMS trains of the audio close-loop system. ECG time series are used to extract the RR-peaks and the amplitude deviations from the overall (estimated) mean amplitude of the R-peaks obtained (mean-shifted data). Then normalization by equation 1 (see Supplementary File, section "Micro-Movement Spikes") is used to obtain the MMS trains. Similar methods are used to handle the audio waveforms and play the song back according to the person's real-time performance.

Figure 6: **Inducing systematic changes in the empirically estimated Gamma PDFs** and their stochastic trajectories of the Four Gamma Moments from the performance under the proxy control using the Audio Close-loop System. (**A**) PDFs from the MMS trains of each of the data type (ECG top and audio file bottom) for each of the dance contexts, spontaneous improvisation and deliberate routine. Legends are Imp Or (improvisation original) denoting the baseline condition at the start of the session; Imp Alt1 denoting the improvisation during alteration 1; Imp Alt2 denoting improvisation during alteration 2. (**B**) Likewise, for the deliberate rehearsed routine, Rout Or means routine original; Rout Alt1 means routine alteration 1; Rout Alt2 means routine alteration 2. The panels in (**C**) show the systematic shifts in Gamma moments as both the audio signals from the songs and those from the heart shift in tandem and in real time.

Figure 7: Results from the non-parametric Kruskal-Wallis and Multiple comparison post hoc tests. The results of the non-parametric ANOVA (Kruskal-Wallis test) applied on the MMS of the heart data to compare the six conditions. The plot demonstrates the multi-comparison of the 6 cases, indicating the significant difference between the "Rout. Or" and "Imp. Or" conditions. The table shows the results of the Kruskal Wallis test.

Figure 8: The visual representation of the Audio-Visual Interface. 1. A motion-capture system is utilized for acquisition of the peripheral kinematic data. 2. The system collects the positions of the sensors (in our example LED's) to estimate the skeleton – position on the bones. 3. The bone positions are then aligned in our MATLAB developed interface using our own forward-kinematics model. 4. The aligned positions are used to map the skeleton information to our 3D rendered avatar. 5. The mapping of the streamed data to the avatar is in real time which creates the sensation of looking at the person's mirrored image.

Figure 9: Empirically estimated Gamma PDFs and Gamma Signatures of the bodily biorhythms during interactions using the Audio-Visual Close-Loop System. Using the MMS trains derived from the speed of the hips of each participant (C1 - C6), we used MLE to fit the best PDF with 95% confidence intervals. Each participant is represented by a different symbol while the conditions are represented by different colors. A family of Gamma PDFs when in the volume (in) differs from that outside the volume (out). Besides the Gamma empirically estimated PDFs, the estimated Gamma shape and scale parameters are also shown for each person on the Gamma parameter plane.

Table 1: Output of the non-parametric ANOAVA-Kruskal-Wallis test. The results of the Kruskal Wallis test comparing the recordings of inside versus outside the RoI for the MMS and the speed data. We apply the test on the data of each participant (C1 - C6) separately.

DISCUSSION

This paper introduces the concept of proxy control via close-loop co-adaptive, interactive, multi-modal interfaces that harness, parameterize and re-parameterize the peripheral signal of the person in the context of dyadic exchange. We aimed at characterizing stochastic shifts in the fluctuations of the person's biorhythms and parameterizing the change. Further we aimed at systematically steering the stochastic signatures of their biorhythms towards targeted levels of noise-to-signal regimes in near real time.

We presented a generic protocol for building a close-loop interface which satisfied 5 core elements: 1) the collection of multiple bodily data coming from the CNS, PNS, and ANS using various instruments and technologies; 2) the synchronized recording and streaming of the data; 3) the real-time analysis of the selected signals; 4) the creation of sensory augmentation (audio, visual, etc.) using physiological features extracted for the bodily signals; and 5) the continuous tracking of the human system and parallel sensory augmentation closes the loop of the interaction between the human and the system.

The generic protocol was applied on two example interfaces. The first one investigates the dyadic exchange between two human agents and the second one between a human and an avatar agent. The two types of dyads were used to provide proof of concept that the peripheral signal can be systematically changed in real time and that these stochastic changes can be precisely tracked. One dyad was composed of two participants physically interacting, while the other involved a participant interacting with a virtual agent in the form of a 3D rendered avatar endowed with the person's motions and with altered variants of these real-time motions. Such alterations were evoked by interactive manipulations driven by auditory and/or visual sensory inputs in a setting of augmented sensations. In both the real dyad and the artificial dyad, we demonstrated the feasibility of remotely shifting the peripheral signals, including bodily biorhythms and autonomic signals from the heartbeat.

We presented new experimental protocols to probe such shifts in efferent motor variability as the kinesthetic signal streams are being manipulated and re-parameterized in near real time. This

re-entrant information (kinesthetic reafference[48]) proved valuable to shift the systems performance in real time. They bear information about the action's sensory consequences, which we can be precisely tracked using the methods that we presented here.

We also showed data types and statistical methods amenable to standardize our analyses. We provided multiple visualization tools to demonstrate the real-time changes in physiological activities naturally evolving in different contexts, with empirically guided statistical inference that lends itself to interpretation of the self-generated and self-controlled nervous systems signals. Importantly, the changes that were evoked by the proxy controller were smooth and yet quantifiable, thus lending support to the notion that peripheral activity is useful in more than one way. While we can implement these methods using commercially available wireless wearable sensors, we can systematically induce changes in performance that are capturable in the biophysical rhythms without, stressing the system. It is important to translate our methods to the clinical arena and use them as a testbed to develop new intervention models (e.g., as when using augmented reality in autism [49]). In such models, we will be able to track and quantify the sensory consequences of the person's naturalistic actions, as the sensory inputs are precisely manipulated, and the output is parameterized and re-parameterized in near real time.

We offer this protocol as a general model to utilize various biorhythmic activities self-generated by the human nervous systems and harnessed non-invasively with wireless wearables. Although we used a set of biosensors to register EEG, ECG and kinematics in this paper, the methods of recording, synchronizing and analyzing the signals are general. The interface can thus incorporate other technologies. Furthermore, the protocols can be modified to include other naturalistic actions and contexts that extend to the medical field. Because we have aimed for natural behaviors, the setup that we have developed can be used in playful settings (e.g., involving children and parents.)

Several disorders of the nervous systems could benefit from such playful approaches to the control problem. In both types of dyadic interactions that we showed here, the participants could aim at consciously controlling the music, while the proxy controller uses the peripheral output to unconsciously manipulate and systematically shift its signatures. Because scientists have spent years empirically mapping the Gamma parameter plane and the corresponding Gamma moments space across different age groups (neonates to 78 years of age)[19,50-53] and conditions (autism, Parkinson's disease, stroke, coma state and deafferentation), for different levels of control (voluntary, automatic, spontaneous, involuntary and autonomic)[25,47,54], they have empirically measured criteria denoting where on the Gamma spaces the stochastic signatures should be for a good predictive control. Previous research has also shown that we know where the parameters are in the presence of spontaneous random noise coming from the self-generated rhythms of the human nervous systems[7,19,55,56]. Within an optimization schema minimizing biorhythmic motor noise, we can thus aim at driving the signals in such a way as to attain the targeted areas of the Gamma spaces where the shape and dispersion signatures of the family of PDFs of each person is conducive of high signal to noise ratio and predictive values. In this sense, we do not lose gross data and rather use it effectively to drive the system towards desirable levels of noise within a given situation.

Dyadic interactions are ubiquitous in clinical or training settings. They may occur between the trainer and the trainee; the physician and the patient; the clinical therapist and the patient; and they may also occur in research settings that involve translational science and engage the researcher and the participant. One of the advantages of the present protocols is that while they are designed for dyads, they also are personalized. As such, it is possible to tailor the co-adaptive interactions to the person's best capabilities and predispositions, according to their ranges of motion, their ranges of sensory processing times and while considering the ranges in signals' amplitude across the functional hierarchy of the person's nervous systems. As the stochastic trajectory emerges and evolves in time, it is also possible to ascertain the rates of chance of the signatures and use that time series to forecast several impending events along with possible sensory consequences.

Finally, close-loop interfaces could be even used in the art world. They could offer performing artists new avenues to generate computationally driven forms of modern dances, technology dances and new forms of visualization and sonification of bodily expression. In such contexts, the dancer's body can be turned into a sensory-driven instrument to flexibly explore different sensory modalities through sonification and visualization of the self-generated biorhythmic activities, as shown by prior work in this area[40,41,43,46]. Such performance could augment the role of a dancer on stage and let the audience experience subtle bodily signals beyond visible movement.

Several aspects of this technology require further development and testing to optimize their use in real-time settings. The synchronous streaming demands high-speed CPU/GPU power and memory capacity to really exploit the notion of gaining time and being a step ahead when predicting the sensory consequences of the ongoing motor commands. Sampling rates of the equipment should be comparable in order to be able to truly align the signals, perform proper sensory fusion and explore the transmission of information through the different channels of the nervous system. These are some of the limitations present in this new interface.

All and all, this work offers a new concept to improve the control of our bodily system while employing subliminal means that nonetheless allow for systematic standardized outcome measurements of stochastic change.

ACKNOWLEDGEMENTS

We thank the students who volunteered their time to help perform this research; Kan Anant and the PhaseSpace Inc. for providing us with images and videos necessary to describe the set up; and Neuroelectronics for allowing us to use material from the channel www.youtube.com/c/neuroelectrics/ and their manuals. We also thank Professor Elizabeth B. Torres for providing the equipment, her contribution in methods, her assistance with the text writing, and for being the Ph.D. advisor of VK during which time VK developed this project. Finally, we would like to thank Professor Thomas Papathomas and the Laboratory of Vision Research for covering the financial expenses of the publication.

DISCLOSURES

Methods covered by US Patent number 10,176,299 B2 “Methods for the Diagnoses and Treatments of Nervous Systems Disorders” to Torres is owned by Rutgers University.

REFERENCES

1 Kawato, M., Wolpert, D. Internal models for motor control. *Novartis Foundation Symposium.* **218**, 291-304; discussion 304-297 (1998).

2 Wolpert, D. M., Kawato, M. Multiple paired forward and inverse models for motor control. *Neural Networks.* **11** (7-8), 1317-1329 (1998).

3 Wolpert, D. M., Miall, R. C., Kawato, M. Internal models in the cerebellum. *Trends in Cognitive Sciences.* **2** (9), 338-347 (1998).

4 Todorov, E., Jordan, M. I. Optimal feedback control as a theory of motor coordination. *Nature Neuroscience.* **5** (11), 1226-1235 (2002).

5 Todorov, E. Optimality principles in sensorimotor control. *Nature Neuroscience.* **7** (9), 907-915 (2004).

6 Torres, E. B. *Theoretical Framework for the Study of Sensori-motor Integration.*, University of California, San Diego (2001).

7 Harris, C. M., Wolpert, Daniel M. Signal-dependent noise determines motor planning. *Nature.* **394** (20), 780-784 (1998).

8 Torres, E. B., Zipser, D. Reaching to Grasp with a Multi-jointed Arm (I): A Computational Model. *Journal of Neurophysiology.* **88**, 1-13 (2002).

9 Carmena, J. M. et al. Learning to control a brain-machine interface for reaching and grasping by primates. *PLoS Biology.* **1** (2), E42 (2003).

10 Hwang, E. J., Andersen, R. A. Cognitively driven brain machine control using neural signals in the parietal reach region. *2010 Annual International Conference of the IEEE Engineering in Medicine and Biology.* **2010** 3329-3332 (2010).

11 Andersen, R. A., Kellis, S., Klaes, C., Aflalo, T. Toward more versatile and intuitive cortical brain-machine interfaces. *Current Biology.* **24** (18), R885-R897 (2014).

12 Contreras-Vidal, J. L. et al. Powered exoskeletons for bipedal locomotion after spinal cord injury. *Journal of Neural Engineering.* **13** (3), 031001 (2016).

13 Choi, K., Torres, E. B. Intentional signal in prefrontal cortex generalizes across different sensory modalities. *Journal of Neurophysiology.* **112** (1), 61-80 (2014).

14 Hwang, E. J., Andersen, R. A. Cognitively driven brain machine control using neural signals in the parietal reach region. *2010 Annual International Conference of the IEEE Engineering in Medicine and Biology.* **2010** 3329-3332 (2010).

15 Andersen, R. A., Kellis, S., Klaes, C., Aflalo, T. Toward more versatile and intuitive cortical brain-machine interfaces. *Current Biology.* **24** (18), R885-R897 (2014).

16 Contreras-Vidal, J. L. et al. Powered exoskeletons for bipedal locomotion after spinal cord injury. *Journal of Neural Engineering.* **13** (3), 031001 (2016).

17 Choi, K., Torres, E. B. Intentional signal in prefrontal cortex generalizes across different sensory modalities. *Journal of Neurophysiology.* **112** (1), 61-80 (2014).

18 Yanovich, P., Isenhower, R. W., Sage, J., Torres, E. B. Spatial-orientation priming impedes rather than facilitates the spontaneous control of hand-retraction speeds in patients with Parkinson's disease. *PLoS One.* **8** (7), e66757 (2013).

19 Torres, E. B., Cole, J., Poizner, H. Motor output variability, deafferentation, and putative deficits in kinesthetic reafference in Parkinson's disease. *Frontiers in Human Neuroscience.* **8** 823 (2014).
20 Torres, E. B. et al. Toward Precision Psychiatry: Statistical Platform for the Personalized Characterization of Natural Behaviors. *Frontiers in Human Neuroscience.* **7**, 8 (2016).
21 Torres, E. B., Cole, J., Poizner, H. Motor output variability, deafferentation, and putative deficits in kinesthetic reafference in Parkinson's disease. *Frontiers in Human Neuroscience.* **8**, 823 (2014).
22 Torres, E. B. et al. Autism: the micro-movement perspective. *Frontiers in Integrative Neuroscience.* **7**, 32 (2013).
23 Ryu, J., Vero, J., Torres, E. B. in *MOCO '17: Proceedings of the 4th International Conference on Movement Computing.* 1-8 (ACM).
24 Brincker, M., Torres, E. B. Noise from the periphery in autism. *Frontiers in Integrative Neuroscience.* **7**, 34 (2013).
25 Torres, E. B. Two classes of movements in motor control. *Experimental Brain Research.* **215** (3-4), 269-283 (2011).
26 Torres, E. B. Signatures of movement variability anticipate hand speed according to levels of intent. *Behavioral and Brain Functions.* **9**, 10 (2013).
27 Gramann, K. et al. Cognition in action: imaging brain/body dynamics in mobile humans. *Reviews in the Neurosciences.* **22** (6), 593-608 (2011).
28 Makeig, S., Gramann, K., Jung, T. P., Sejnowski, T. J., Poizner, H. Linking brain, mind and behavior. *International Journal of Psychophysiology.* **73** (2), 95-100 (2009).
29 Ojeda, A., Bigdely-Shamlo, N., Makeig, S. MoBILAB: an open source toolbox for analysis and visualization of mobile brain/body imaging data. *Frontiers in Human Neuroscience.* **8**, 121 (2014).
30 Casadio, M. et al. in *IEEE International Conference on Rehabilitation Robotics.* (ed IEEE) (IEEE Xplore).
31 Pierella, C., Sciacchitano, A., Farshchiansadegh, A., Casadio, M., Mussaivaldi, S. A. in *7th IEEE International Conference on Biomedical Robotics and Biomechatronics.* (IEEE Xplore).
32 Torres, E. B. Two classes of movements in motor control. *Experimental Brain Research.* **215** (3-4), 269-283 (2011).
33 Purves, D. *Neuroscience*. Sixth edition. edn (Oxford University Press, 2018).
34 Torres, E. B. Signatures of movement variability anticipate hand speed according to levels of intent. *Behavioral and Brain Functions.* **9**, 10 (2013).
35 Torres, E. B. The rates of change of the stochastic trajectories of acceleration variability are a good predictor of normal aging and of the stage of Parkinson's disease. *Frontiers in Integrative Neuroscience.* **7**, 50 (2013).
36 Torres, E. B., Vero, J., Rai, R. Statistical Platform for Individualized Behavioral Analyses Using Biophysical Micro-Movement Spikes. *Sensors (Basel).* **18** (4) (2018).
37 Torres, E. B. in *Progress in Motor Control* 229-254 (Springer, 2016).
38 Torres, E. B., Yanovich, P., Metaxas, D. N. Give spontaneity and self-discovery a chance in ASD: spontaneous peripheral limb variability as a proxy to evoke centrally driven intentional acts. *Frontiers in Integrative Neuroscience.* **7**, 46 (2013).
39 Gramann, K., Jung, T. P., Ferris, D. P., Lin, C. T., Makeig, S. Toward a new cognitive

neuroscience: modeling natural brain dynamics. *Frontiers in Human Neuroscience.* **8**, 444 (2014).
40 Kalampratsidou, V., Torres, E. B. Bodily Signals Entrainment in the Presence of Music. *Proceedings of the 6th International Conference on Movement and Computing.* 3 (2019).
41 Kalampratsidou, V., Torres, E. B. Sonification of heart rate variability can entrain bodies in motion. *Proceedings of the 7th International Conference on Movement and Computing.* 10.1145/3401956.3404186 Article 2 (2020).
42 Kalampratsidou, V. *Co-adaptive multimodal interface guided by real-time multisensory stochastic feedback*, Rutgers University-School of Graduate Studies (2018).
43 Kalampratsidou, V., Kemper, S., Torres, B., Elizabeth. Real time streaming and closed loop co-adaptive interface to steer multi-layered nervous systems performance. *48th Annual Meeting of Society for Neuroscience.* (2018).
44 Kalampratsidou, V., Torres, E. B. Body-brain-avatar interface: a tool to study sensory-motor integration and neuroplasticity. *Fourth International Symposium on Movement and Computing, MOCO.* **17** (2017).
45 Kalampratsidou, V., Torres, E. B. Peripheral Network Connectivity Analyses for the Real-Time Tracking of Coupled Bodies in Motion. *Sensors (Basel).* **18** (9) (2018).
46 Kalampratsidou, V., Zavorskas, M., Albano, J., Kemper, S., Torres, E. B. Dance from the heart: A dance performance of sounds led by the dancer's heart. *Sixth International Symposium on Movement and Computing.* (2019).
47 Kalampratsidou, V., Torres, E. B. Outcome measures of deliberate and spontaneous motions. *Proceedings of the 3rd International Symposium on Movement and Computing.* 9 (2016).
48 Von Holst, E., Mittelstaedt, H. in *Perceptual Processing: Stimulus equivalence and pattern recognition* (ed P.C. Dodwell) 41-72 (Appleton-Century-Crofts, 1950).
49 Torres, E. B., Yanovich, P., Metaxas, D. N. Give spontaneity and self-discovery a chance in ASD: spontaneous peripheral limb variability as a proxy to evoke centrally driven intentional acts. *Frontiers in Integrative Neuroscience.* **7**, 46 (2013).
50 Torres, E. B. *Objective Biometric Methods for the Diagnosis and Treatment of Nervous System Disorders*. (Academic Press, Elsevier, 2018).
51 Torres, E. B. et al. Toward Precision Psychiatry: Statistical Platform for the Personalized Characterization of Natural Behaviors. *Frontiers in Neurology.* **7**, 8 (2016).
52 Wu, D. et al. How doing a dynamical analysis of gait movement may provide information about Autism. *APS March Meeting Abstracts.* (2017).
53 Torres, E. B. et al. Characterization of the statistical signatures of micro-movements underlying natural gait patterns in children with Phelan McDermid syndrome: towards precision-phenotyping of behavior in ASD. *Frontiers in Integrative Neuroscience.* **10**, 22 (2016).
54 Kalampratsidou V, T. E. Peripheral Network Connectivity Analyses for the Real-Time Tracking of Coupled Bodies in Motion. *Sensors.* (2018).
55 Brincker, M., Torres, E. B. Noise from the periphery in autism. *Frontiers in Integrative Neuroscience.* **7**, 34 (2013).
56 Torres, E. B., Denisova, K. Motor noise is rich signal in autism research and pharmacological treatments. *Scientific Reports.* **6**, 37422 (2016).

881

Figure

Click here to access/download;Figure;Figure 1.pdf

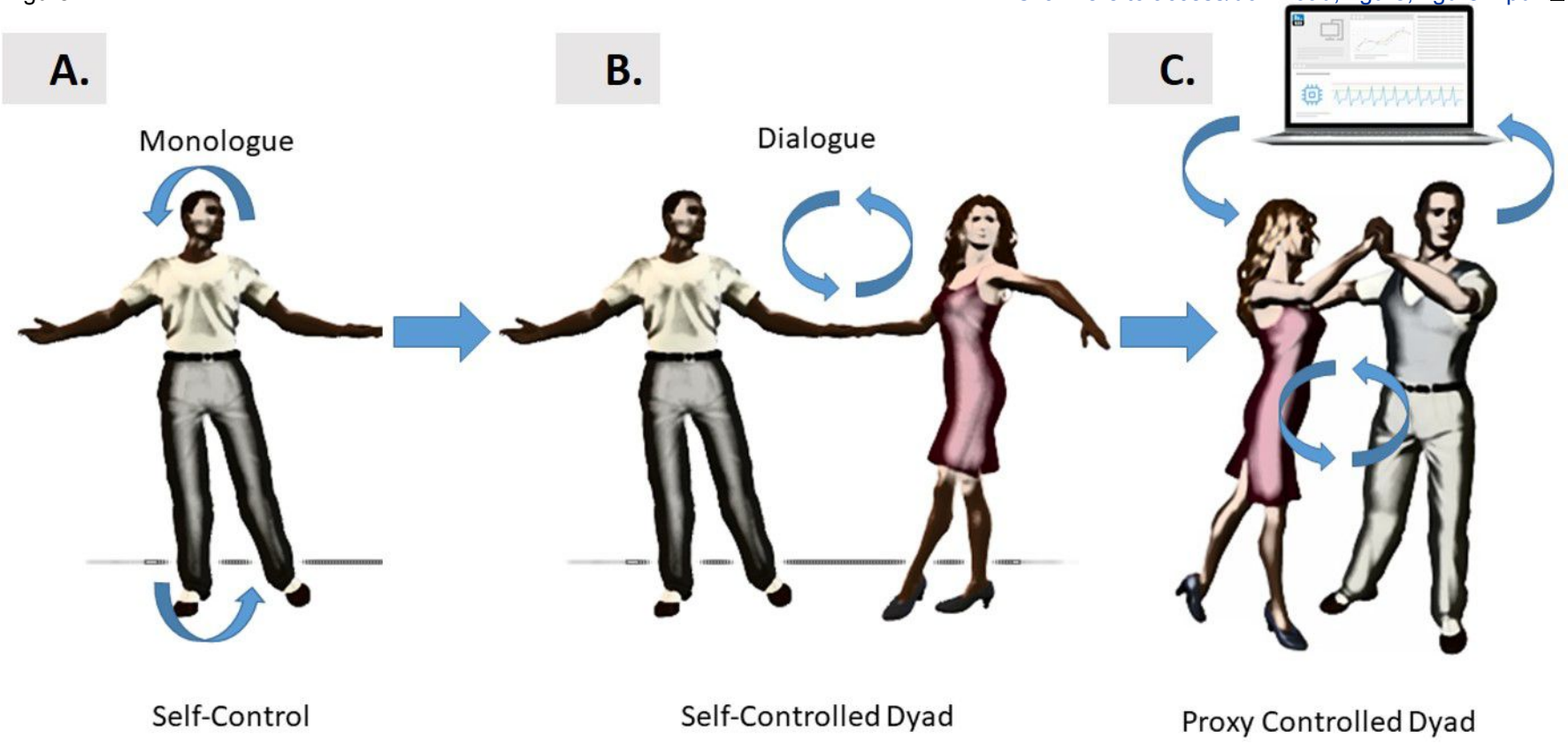

Figure

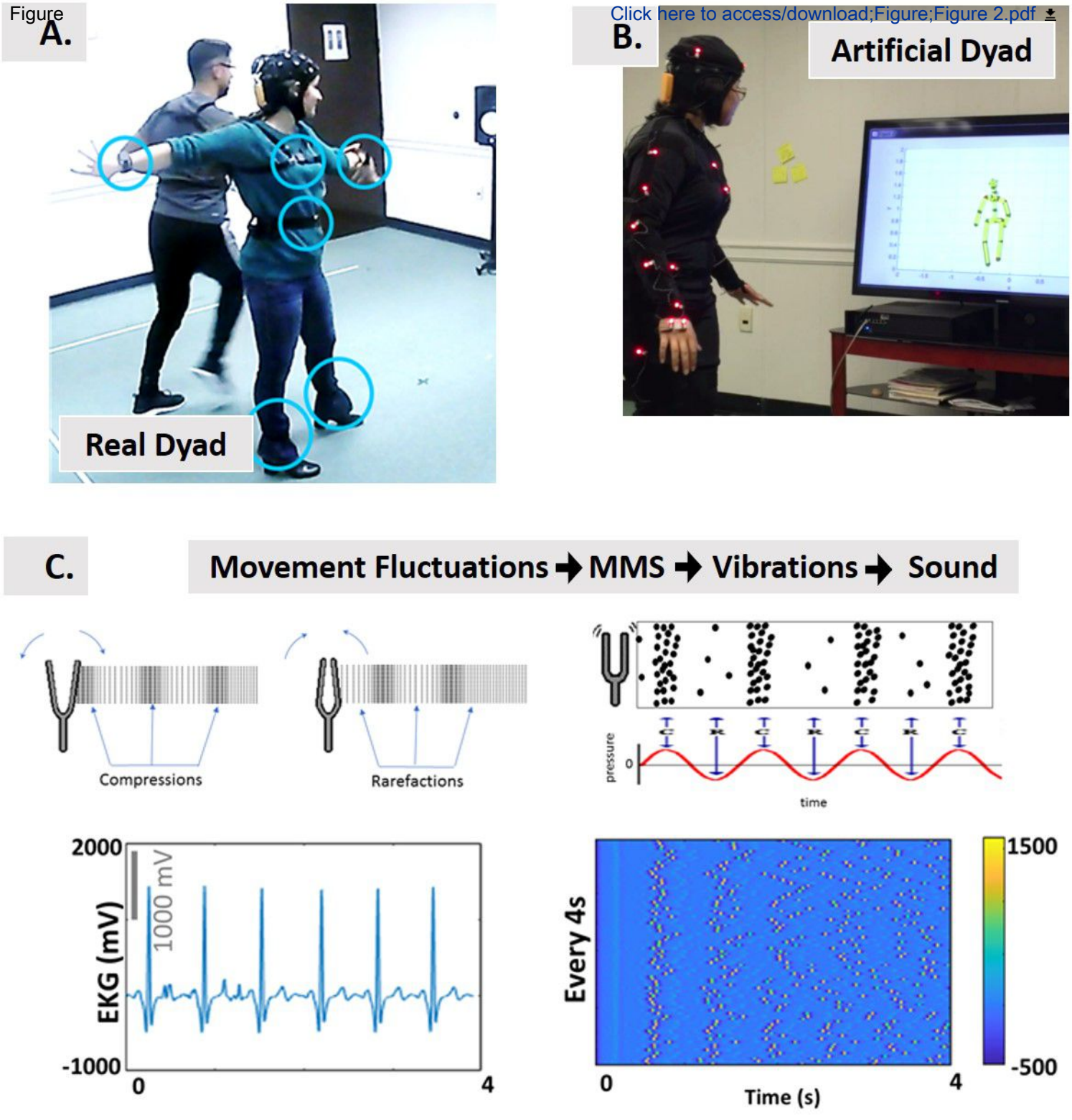

Figure

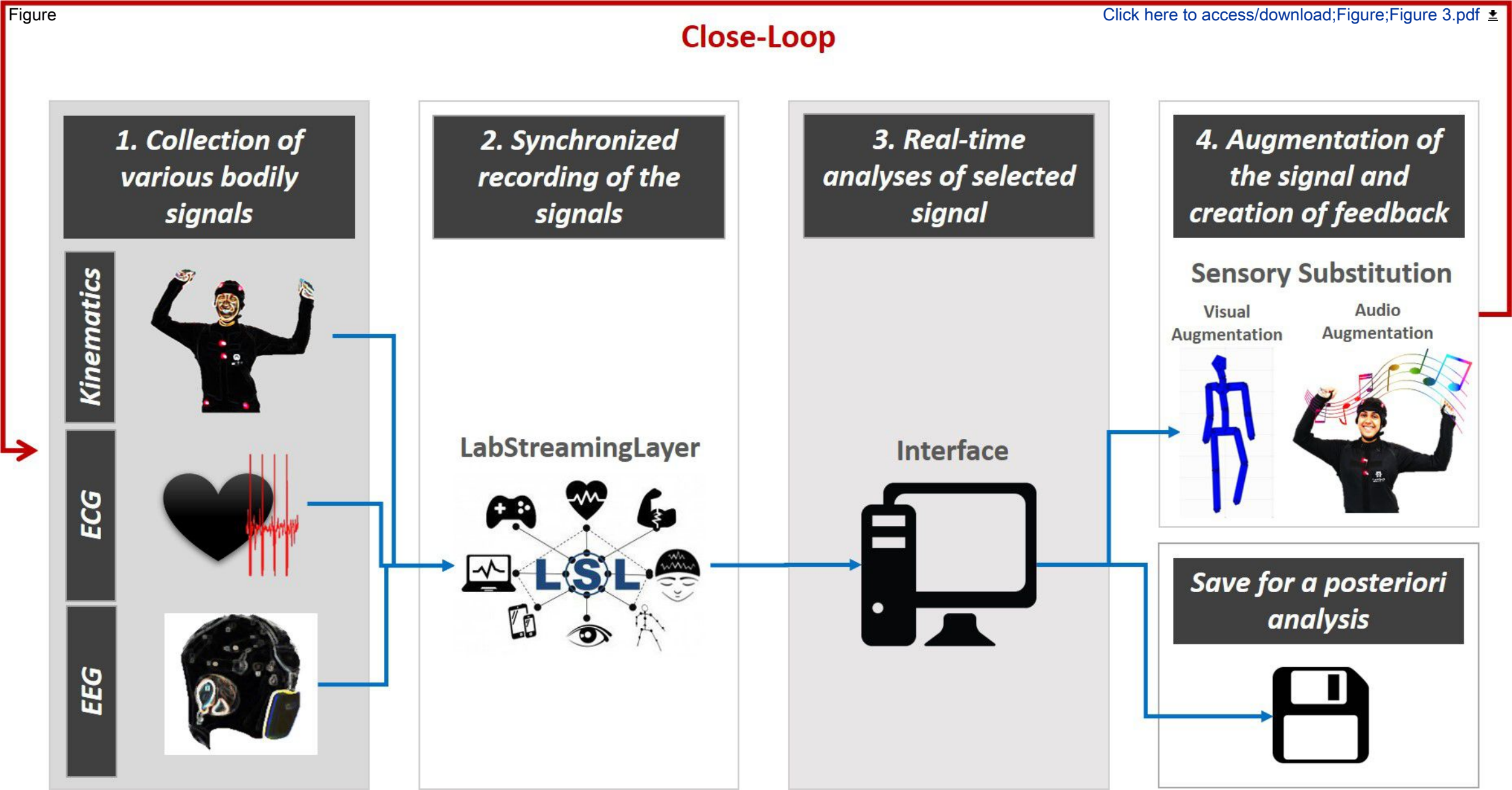

Figure

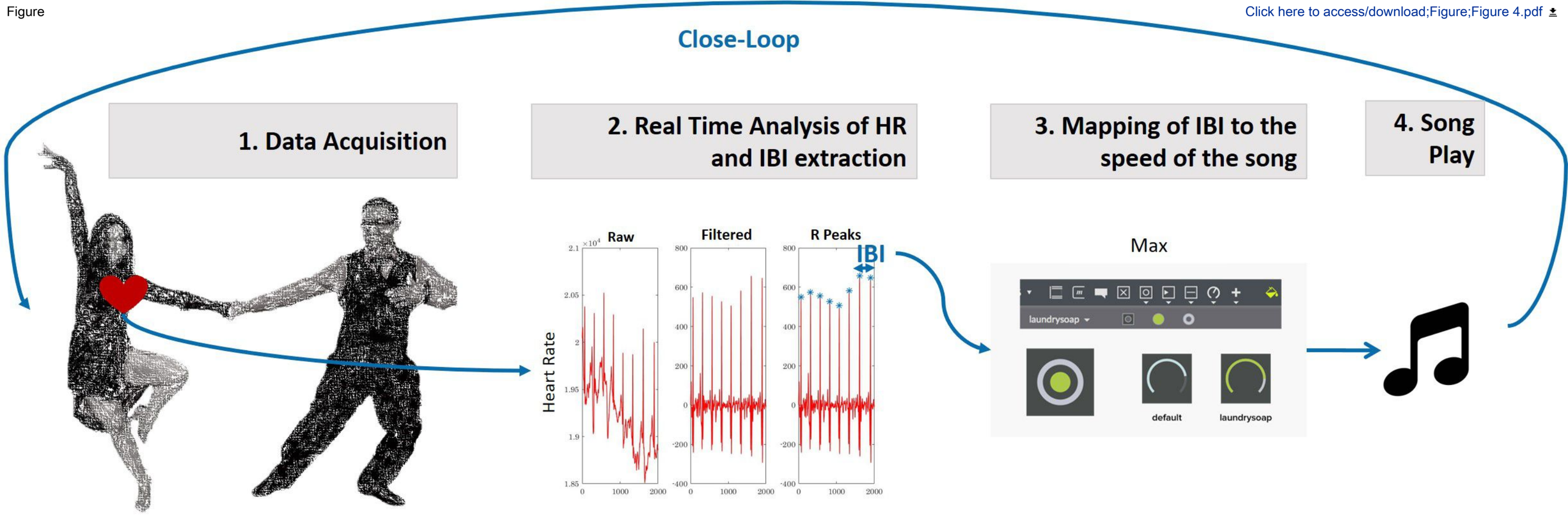

Figure

Click here to access/download;Figure;Figure 5.pdf

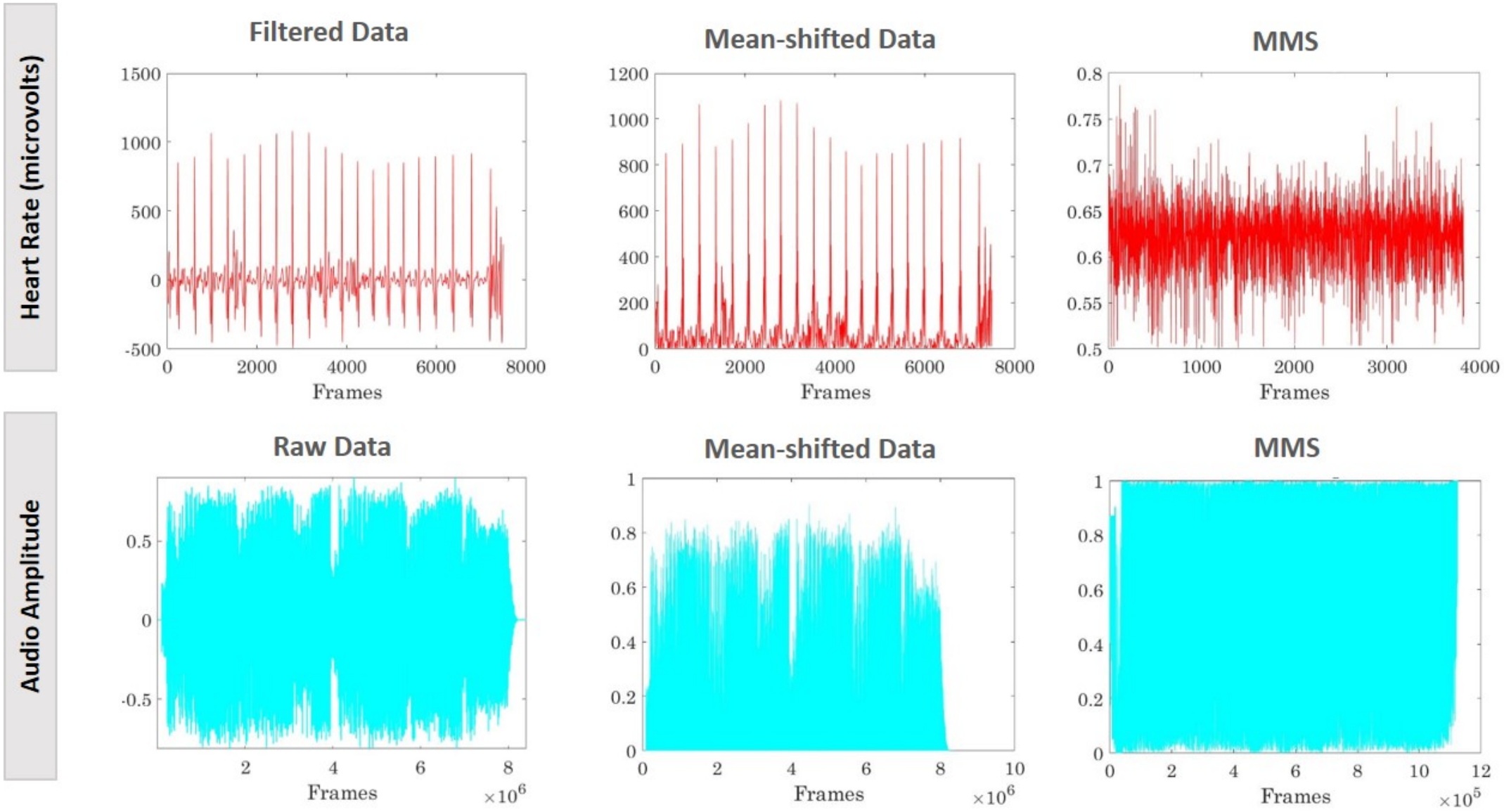

Figure 6

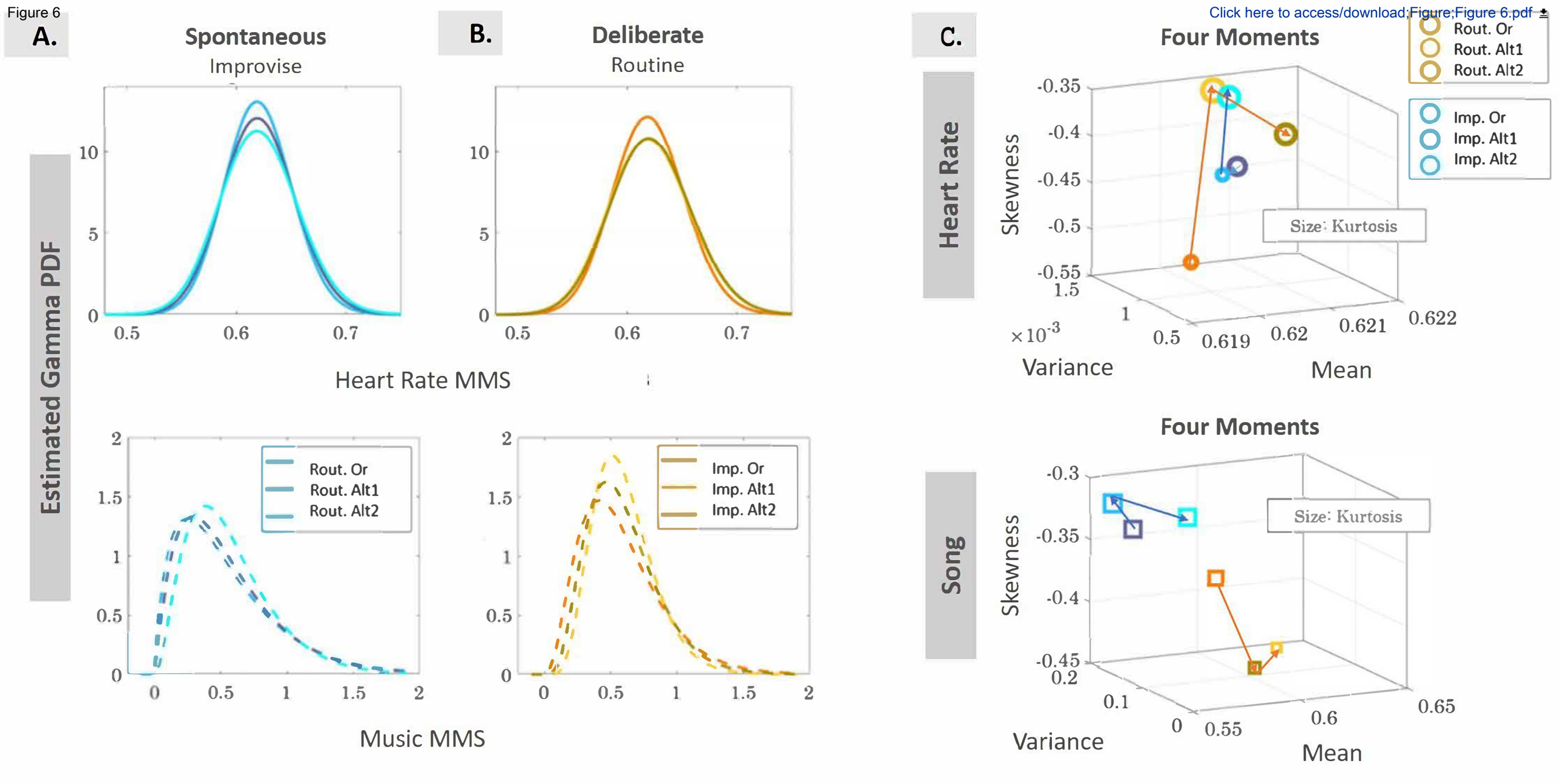

Figure

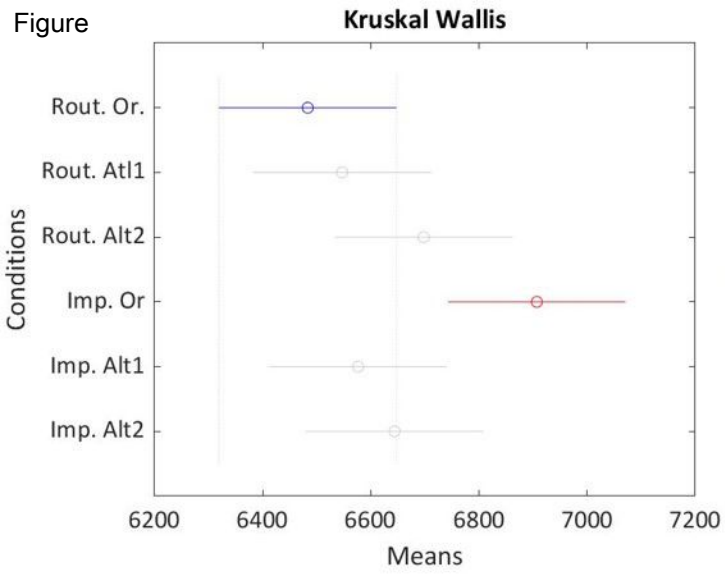

Click here to access/download;Figure;Figure 7.pdf

Kruskal-Wallis ANOVA Table

Source	SS	df	MS	Chi-sq	Prob>Chi-sq
Columns	2.47474e+08	5	4.94948e+07	16.83	0.0048
Error	1.95099e+11	13278	1.46934e+07		
Total	1.95346e+11	13283			

Figure

1. Data acquisition

2. Skeleton of Recap software, PhaseSpace

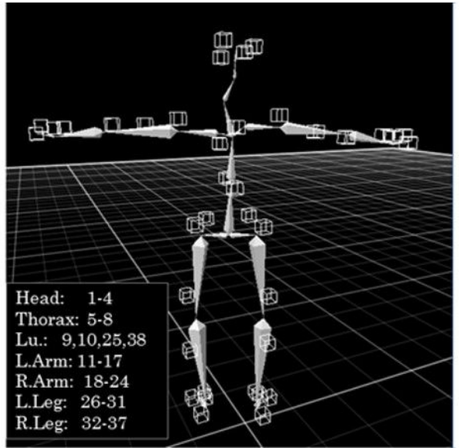

3. Bone positions transferred in Matlab

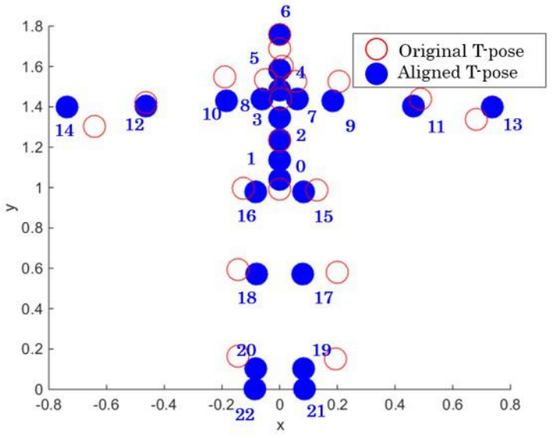

4. Matlab developed avatar

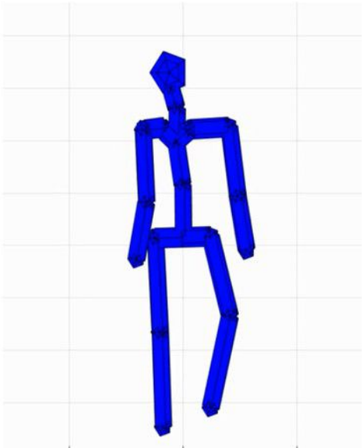

5. 3D Real-time representation in Matlab

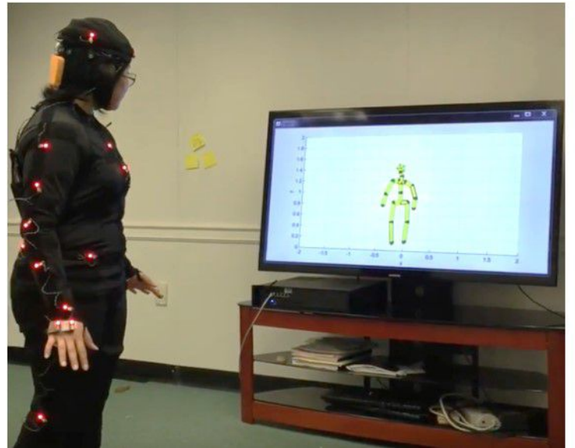

Figure

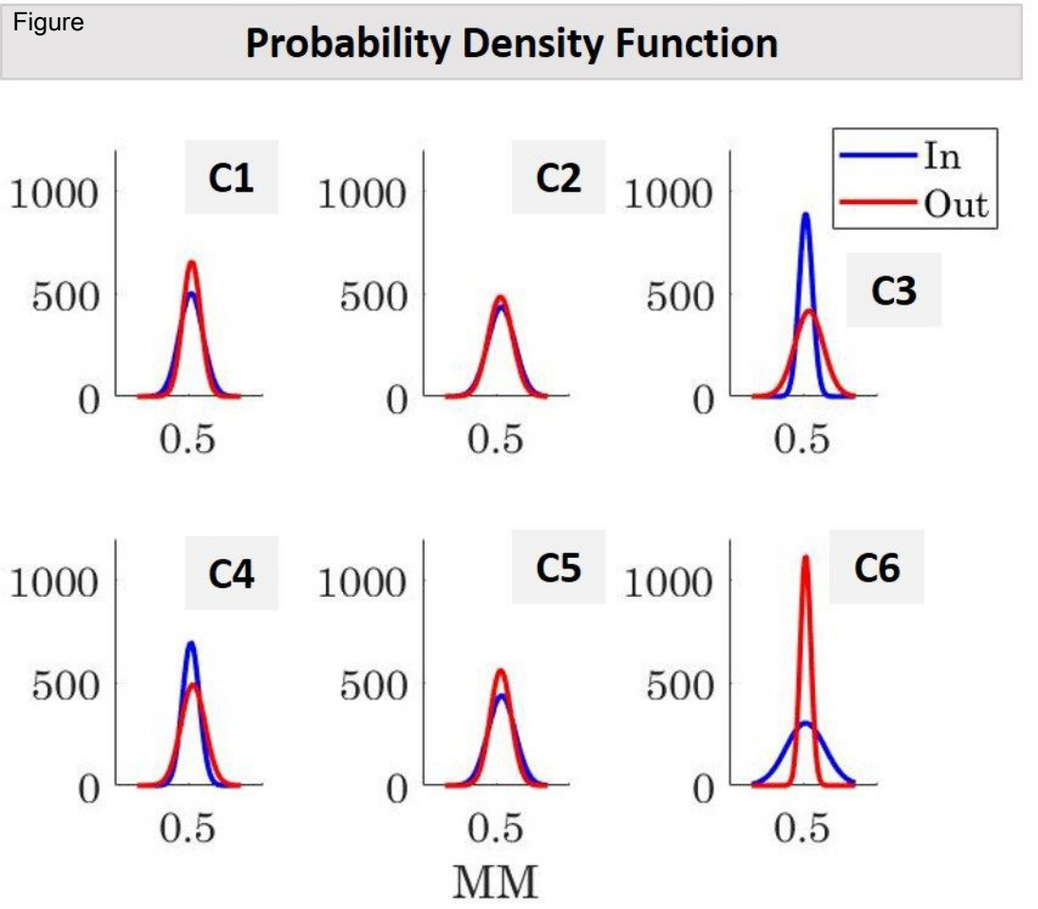

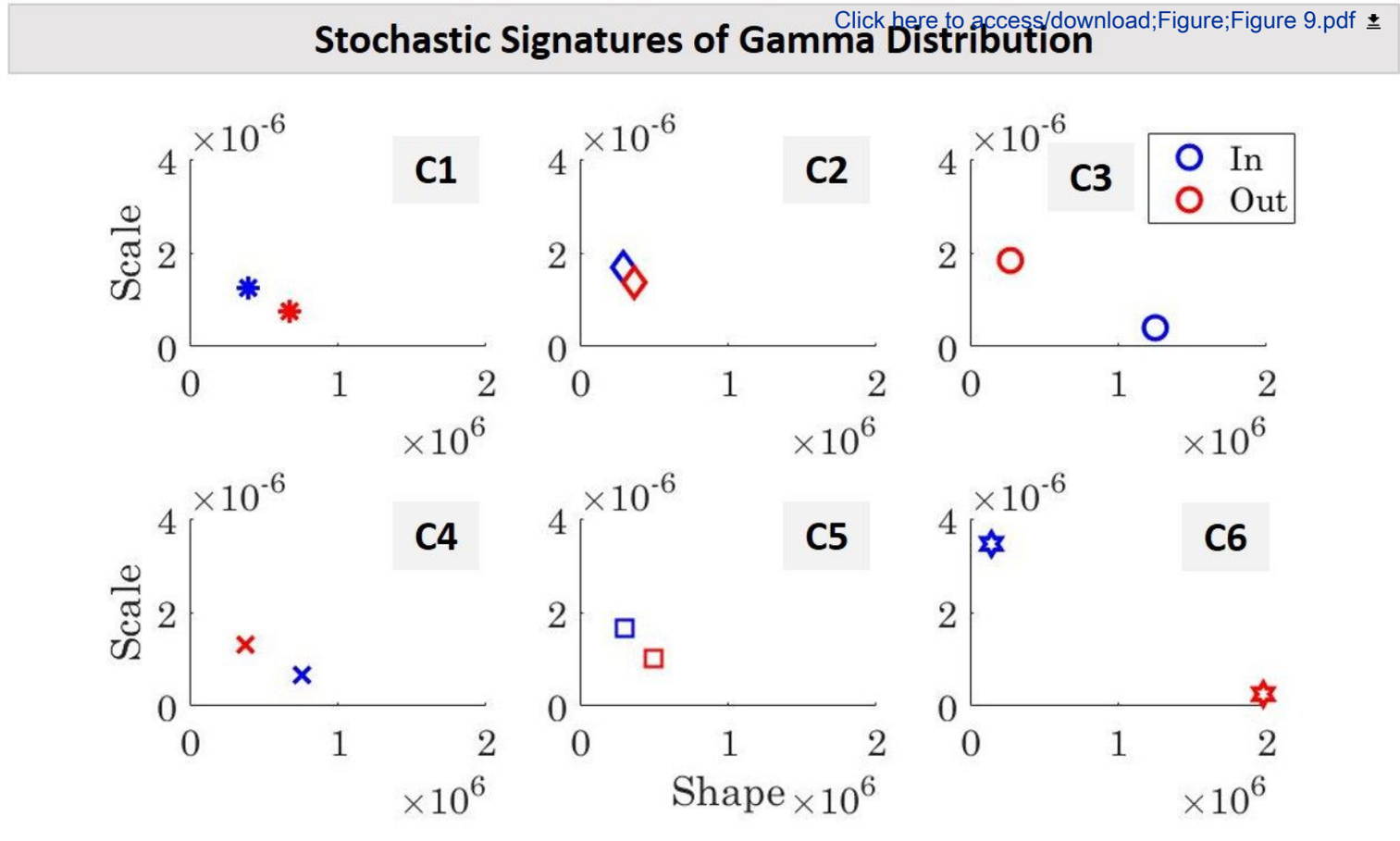

Table 1

Kruskal Wallis Test	Speed data	MMS
C1	0	1.34 e-05
C2	0	4.72E-15
C3	0	8.59E-34
C4	2.70E-21	3.16E-04
C5	0	1.11E-09
C6	0	5.95E-05

Table

Click here to access/download;Table;sup-Table1.xlsx

Song	Duration
Imp. Or	3 min 10 s
Imp. Alt1	2 min 1 s
Imp. Alt2	2 min 33 s
Rout. Or	2 min 50 s
Rout. Alt1	2 min 7 s
Rout. Alt2	2 min 55 s

Table of Materials

Click here to access/download;Table of Materials;JoVE_Materials.xlsx

Name of Material/ Equipment	Company	Catalog Number	Comments/Description
Enobio 32	Enobio		Hardware for EEG data collection
Enobio ECG Extention	Enobio		Hardware for ECG data collection
LabStreamingLayer (LSL)			Synchronization and streaming of data
Matlab	Mathwork		Analysis and processing of data
Max	Cycling'74		Sonification of bodily information
NIC.2	Enobio		Software for EEG and ECG data collection
PhaseSpace Impulse	PhaseSpace		Hardware for collection of the kinematic data (position, speed, acceleration)
Python3	Python		Analysis and processing of data
Recap	PhaseSpace		Software for collection of the kinematic data (position, speed, acceleration)

Dear Editorial Board,

We would like to thank you for your comments on our video and manuscript. Below you will find our responses to your comments.

Editorial and production comments:
Changes to be made by the Author(s) regarding the written manuscript:
1. Please take this opportunity to thoroughly proofread the manuscript to ensure that there are no spelling or grammar issues.

We took the time to thoroughly proofread the manuscript before the final submission.

Changes to be made by the Author(s) regarding the video:
1. Audio & Narration
• 00:48 - 00:48 I can hear **mouse clicks** as if the narrator is reading along to a slide show and advancing the slides as they go along. The clicking can be removed with some more precise editing. We re-recorded the introduction to handle such issues.
• 01:12 - 01:12 The **music** may be too distracting. You may want to lower the volume of the music over this part so we can still hear the narration. We lowered the the volume of the music.
• 01:31 - 01:31 Interview audio is too low compared to the narration. Please refer to the ASV criteria sheet: Audio volume peaks should fall between -12 and -6 dB. We re - recorded the interviews
• 07:18 - 07:18 There is a glitch in the audio when the person goes from full screen to picture in picture. Please remove this audio glitch. This was corrected.
• 00:46 - 00:46 There's a bit of a stumble here, could be edited out or rerecorded. This was corrected.
• 05:17 - 05:17 The audio buzzes here when the person speaks at this point in time. This was corrected.
• 05:46 - 05:46 The person repeats the word streaming, please remove one of the repeated words. This was corrected.
2. Composition
• 00:29 - 00:29 Resize this figure so there's no black border around the frame. The video was updated.
• 02:46 - 02:46 Resize this figure so there's no black border around the frame. The video was updated.
• 03:07 - 03:07 The highlighting of the screen is great, but we can't see exactly what it's highlighting. To help with this, it's better to zoom in on the screen recording in order to view the smaller text. We worked our best to improve this issue, given that the videos did not have a good analysis.
• 07:19 - 07:19 The person speaking doesn't need to be seen. You can get rid of the picture in picture in the lower left so we can focus more on the screen capture. This was corrected.
3. Pacing
• 01:55 - 01:55 There is a cut between two sentences that can be covered with figures or footage that was already filmed. This was corrected.

• 09:27 - 09:27 Narration pauses awkwardly. remove this gap. This was corrected.
• 10:32 - 10:32 The narration sounds like it cuts itself off at the end of the word here. This was corrected.
Space it out so we have time to digest the sentence.

4. Text

• The section titles should be centered top to bottom. Also try to place the title on one line. If it can't fit on one line, try to make each line have an even amount of words. The text was updated.
• 01:33 - 01:33 The person caption name should be bigger in size or bold compared to the university name. There is no functionality to resize part of the text our video Editor, so we capitalized the name-letters.
• 2:53: Set up instead of setup. The text was updated
• 07:12 - 07:12 Person caption should appear again. The text was updated
• 11:29 - 11:29 Person caption needs to reappear here. The text was updated NE

We uploaded the new version of the video here:
https://www.dropbox.com/request/Zg88NzDhWiVCwy60Alzx?oref=e

We appreciate your time and effort.

Sincerely,

Vilelmini Kalampratsidou

Dear Reviewer#1,

We would like to thank your for taking the time to review our manuscript. From your review, there are not any major and mirror suggestions for us.

Reviewer #1:

Manuscript Summary:

The Study present an interesting concept of closed-loop adaptive interface. They present data of a dyadic interaction between two real persons or between a person and an avatar and showed that closing the loop they were able to influence and modify the movement variability of the dyad. The protocol and the set-up are well presented and clear to understand not only from the written text but also from the figures.

I think the manuscript is ready for publication

Major Concerns:

NA

Minor Concerns:

NA

Thank you for positive comments!

Sincerely,

Vilelmini Kalampratsidou

Dear Editorial Board,

We would like to thank you for your comments and suggestions on our manuscript. Bellow you will find our responses to your review comments individually.

Reviewer #2:
Manuscript Summary:
This manuscript by Kalampratsidou and Kemper describes a closed-loop interface platform to provide real-time sensory feedback of monitored signals -motion-capture, EEG, and ECG-during human movement. The methods described are useful and applicable to an interesting line of research with many possibilities. I think the description and methods will be useful to researchers. However, the work could be considerably improved by editing to make clear the setup and results especially in the introduction and write-up related to example 1. Additionally, while the results show statistically significant differences, it's difficult to determine if these are meaningful differences and it is also not intuitive to interpret the results as many of the differences shown are change in the distribution of observations rather than mean shifts. Overall, I think this work is a useful for its technical achievement but the general concept as presented with the specific examples don't do that much to advance the field. That's perhaps ok for this type of work but I think additional editing is needed to clarify both the current results and how that more directly relates to the general idea.

Major Concerns:
The introduction is very abstract at places and a bit disjointed. It would be useful if each paragraph was more explicitly linked to the current setup and application. There is too much that is broad and doesn't set the reader up for what will actually be presented with the current work.

The changes in introduction have been tracked.

Line 453 - In example 1, it's unclear to me what is meant by alteration 1 and 2 and should be written more explicitly with the descriptions in the previous paragraph. Then it's unclear if there's any expectation of what shifts in behavior are expected to occur systematically or if the take home point is just that they are different. In the legend of Fig. 6 it says the audio signals and the heart signals shift in tandem. Yet, it's unclear if the different data points are supposed to somehow line up in the two plots in Fig. 6c; I don't see anything that suggests the shifts are in tandem.

To clarify what is alteration 1 and 2, we added new text in lines 426-428. The finding here is that the shifts are towards the same direction which is emphasized with some new text in lines 466-468. Some further explanation of the result can be found in the video too.

Minor Concerns:
Line 24 - Summary - it is unclear to me what is meant by re-parameterize in addition to parameterize. It's described a little later but especially in the summary it's difficult to understand what is meant.

Summary was updated based on the suggestions of the reviewer.

Line 83 - "cite" should likely be removed

"Cite" was removed.

Line 119 - Purposeful actions have consequences, with precisely characterized motor signatures that are context-dependent and enable inference of levels of mental intent with high certainty.
This sentence is difficult to understand

We corrected the sentence so as to be understood.

Line 182 - "less stressful to the system" is ambiguous to what system is referred to

The text now says "less stressful to the **human** system."

Line 230 - A list of the components or additional introduction would be useful before jumping into the steps

Unfortunately, the template and guidelines of the protocol does not allow us to add any extra text there. The list of the components was submitted as a separate file, as we were advised by the editorial committee. Also, more introductory details can someone locate in section" Building the Interface" which is right above the protocol.

Line 491 Example 1, I believe this is actually Example 2

We updated the number.

Supplemental figures seem have numbers that don't line up between text and figures.

There is text in the supplementary file that says **[Place supplementary Figure # here]** in 3 places**.** In the supplementary file there are references in the figures of the main text which is done by saying "see **Figure #** of the main text" and there are references to the supplementary figures which are mentioned as "see **Supplementary Figure #".**

Thank you for your time.

Sincerely,

Vilelmini Kalampratsidou

Supplementary Figure 1

Click here to access/download;Supplemental File (Figures, Permissions, etc.);sup-Figure 1 conditions.pdf

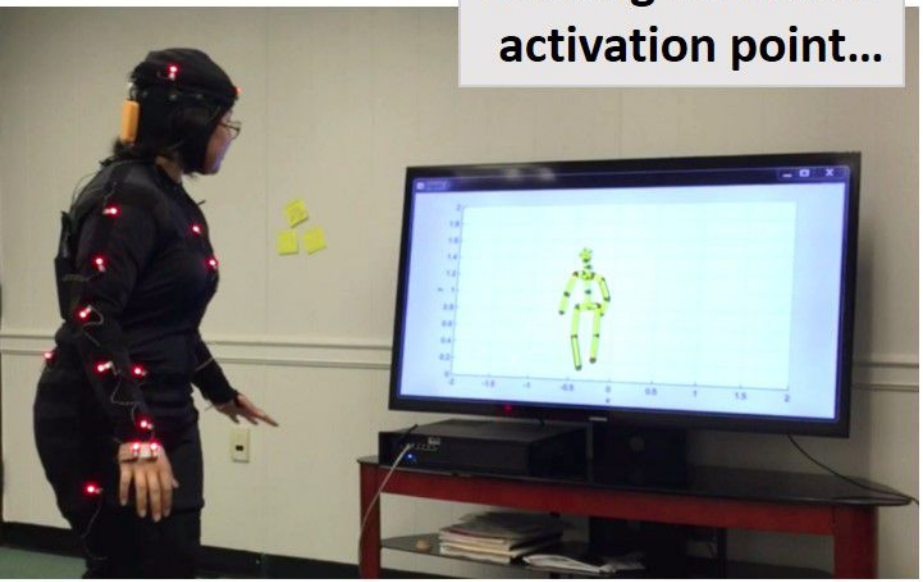

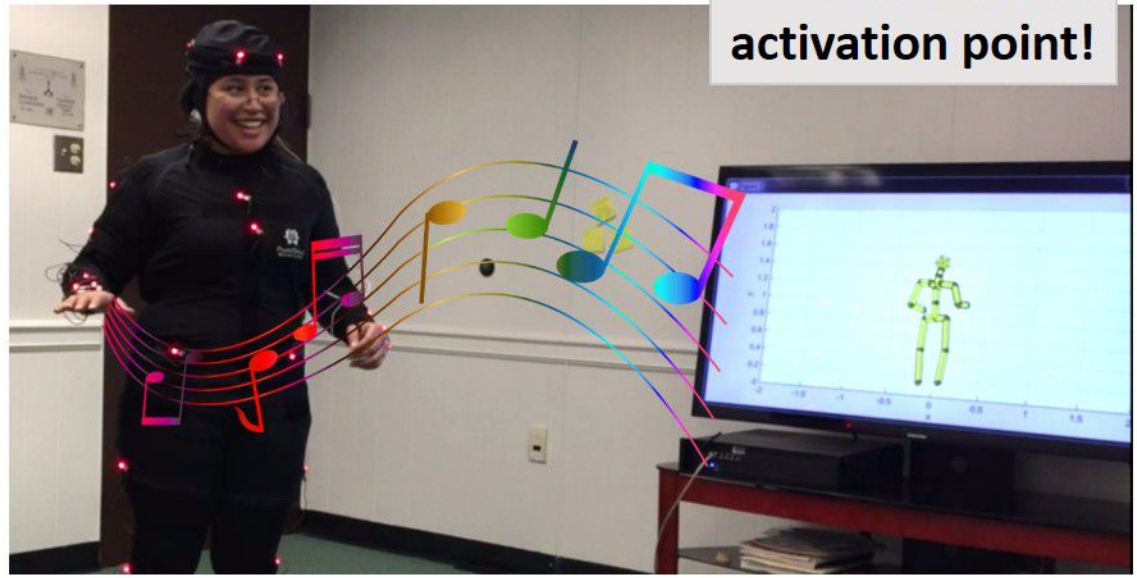

	Criteria	Controller	Controlee
Cond. 1	Position (radius: 50cm)	Hip	Activation of the song
Cond. 2	Position (radius: 50cm)	Hip Right wrist	Activation of the song Sampling rate of the song
Cond. 3	Speed	Hip	Sampling rate of the song

Supplementary Figure 2

Click here to access/download;Supplemental File (Figures, Permissions, etc.);sup-Figure 2 MLE.pdf

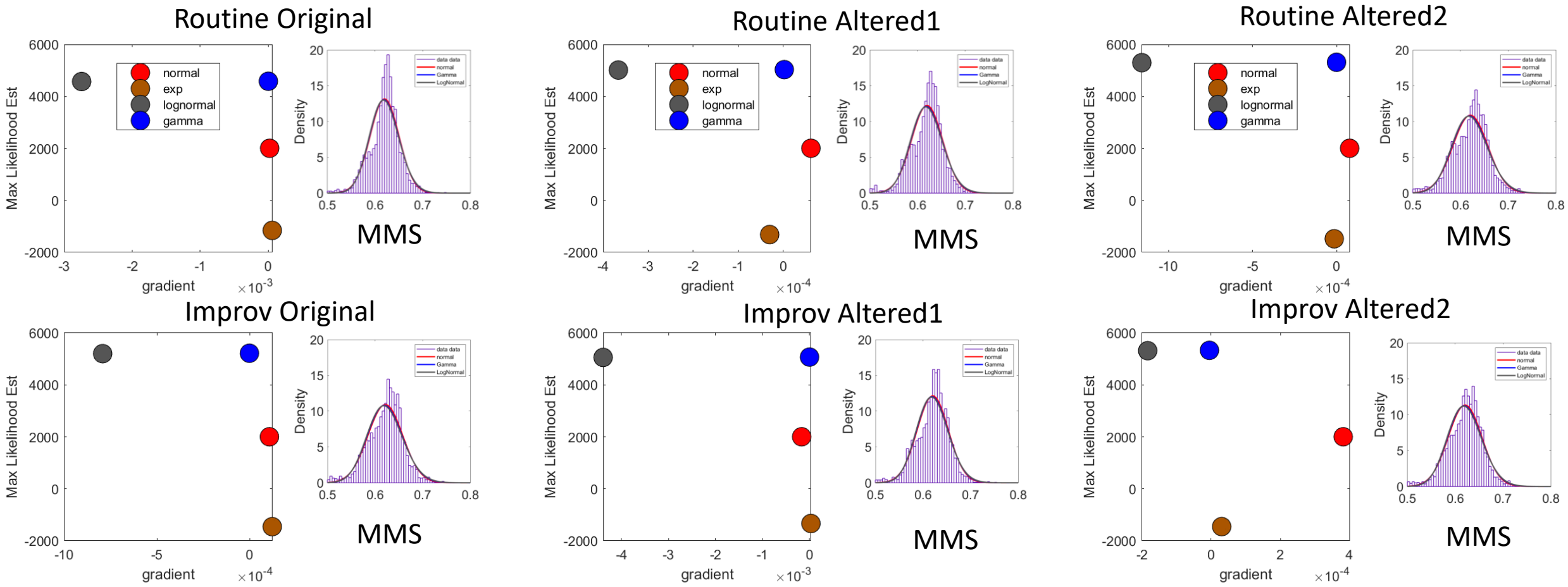

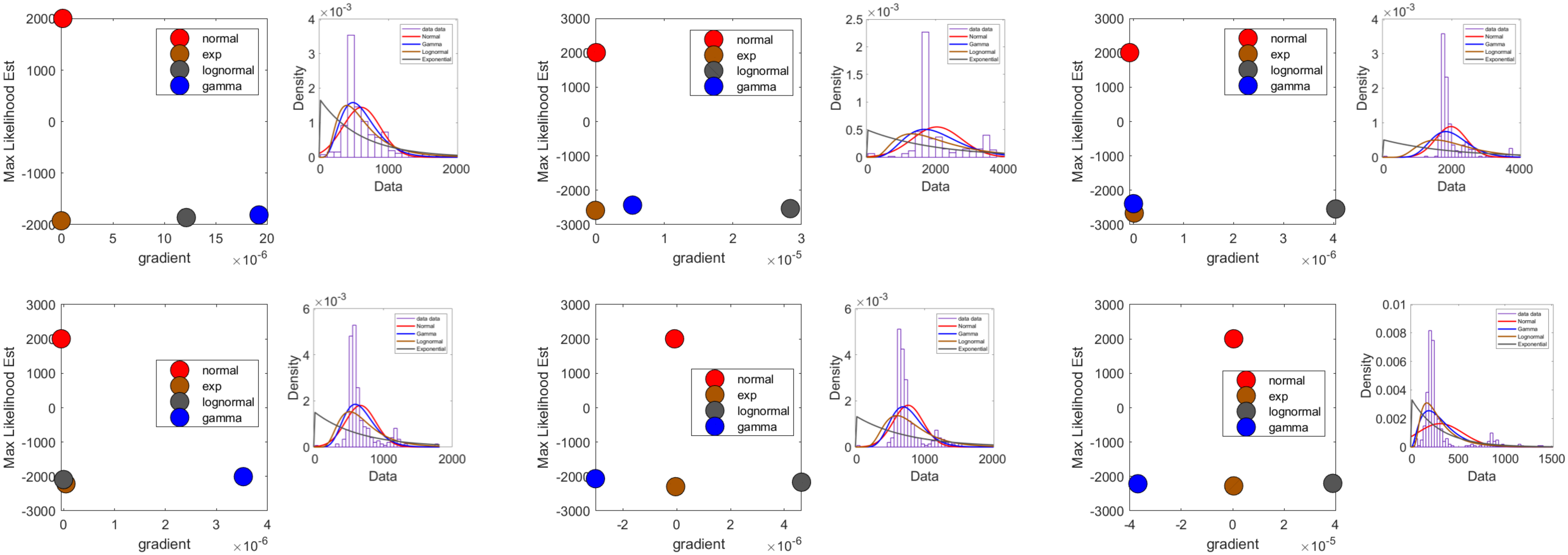

Max Likelihood Est
gradient
×10^-6
normal
exp
lognormal
gamma
Density
Data
×10^-3
data data
Normal
Gamma
Lognormal
Exponential
Max Likelihood Est
gradient
×10^-5
normal
exp
lognormal
gamma
Density
Data
×10^-3
data data
Normal
Gamma
Lognormal
Exponential
Max Likelihood Est
gradient
×10^-6
normal
exp
lognormal
gamma
Density
Data
×10^-3
data data
Normal
Gamma
Lognormal
Exponential
Max Likelihood Est
gradient
×10^-6
normal
exp
lognormal
gamma
Density
Data
×10^-3
data data
Normal
Gamma
Lognormal
Exponential
Max Likelihood Est
gradient
×10^-6
normal
exp
lognormal
gamma
Density
Data
×10^-3
data data
Normal
Gamma
Lognormal
Exponential
Max Likelihood Est
gradient
×10^-5
normal
exp
lognormal
gamma
Density
Data
data data
Normal
Gamma
Lognormal
Exponential

Supplementary Figure 3

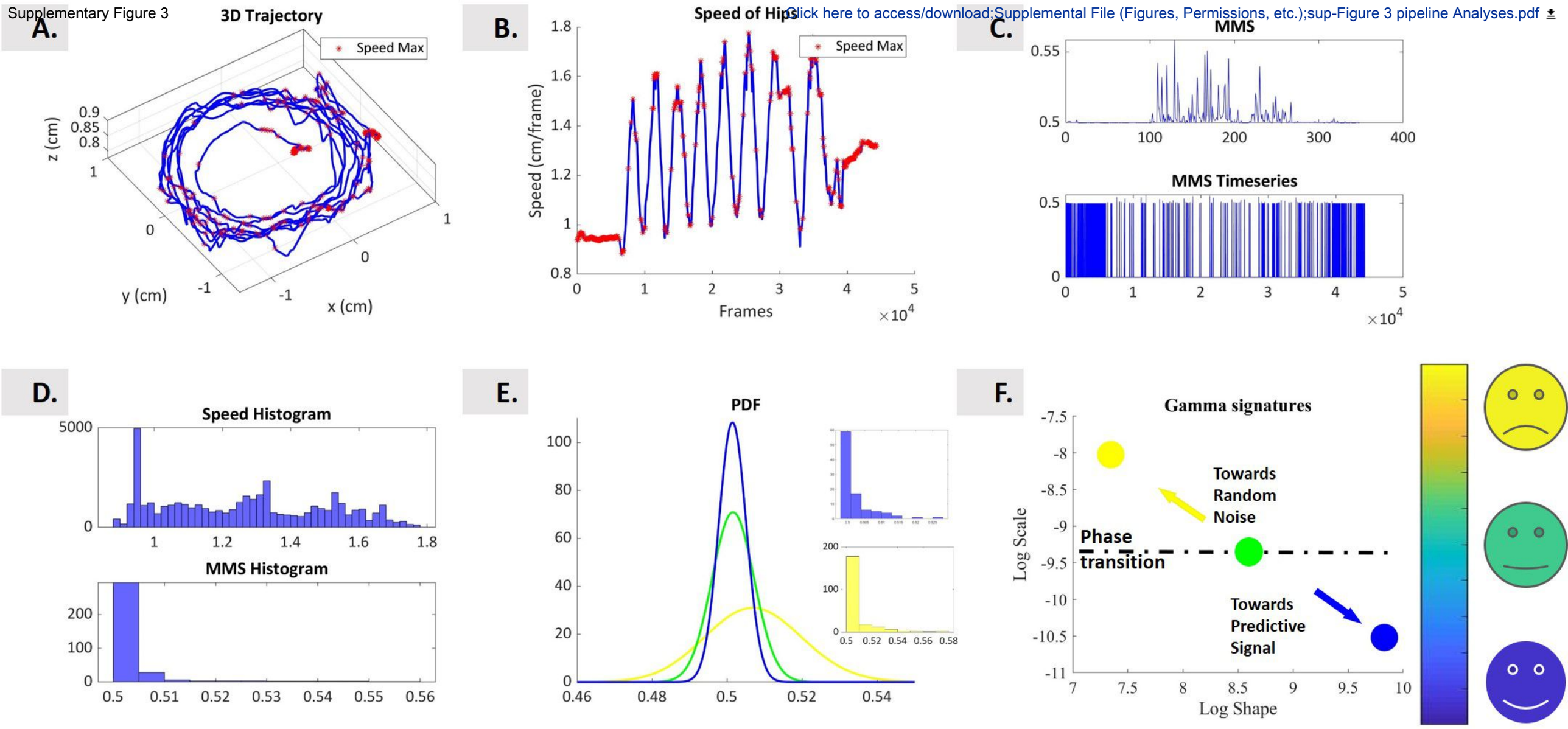

JOURNAL OF VISUALIZED EXPERIMENTS
1 Alewife Center #200
Cambridge, MA 02140
tel. 617.945.9051
www.jove.com

TITLE

Supplementary Material of "Real-Time Proxy-Control of Re-Parameterized Peripheral Signals Using a Close-Loop Interface"

AUTHORS AND AFFILIATIONS

Vilelmini Kalampratsidou[1, 2], Steven Kemper[3]

[1]Center for Cognitive Science, Rutgers University, New Brunswick, NJ, USA
[2]Department of Computer Science, Rutgers University, New Brunswick, NJ, USA
[3]Music Department, Mason Gross School of the Arts, Rutgers University, New Brunswick, NJ, USA

Email Addresses of Authors:
Vilelmini Kalampratsidou, vilelmini.kalabratsidou@gmail.com
Steven Kemper, skemper@mgsa.rutgers.edu

VARIATIONS OF THE PRESENTED CLOSE-LOOP INTERFACE

The design of the generic interface presented in the main text is based on the equipment provided. However, several instruments can be used to register the biophysical signals and replace the sample equipment described above. We acquire brain (Central Nervous System, CNS) signals, bodily kinematics (Peripheral Nervous System, PNS) signals and heart (Autonomic Nervous System, ANS) signals.

Furthermore, LSL (LabStreamingLayer, https://github.com/sccn/labstreaminglayer) is an open access platform that allows the synchronized collection of data that is streaming from various equipment in near real-time. Although in our design the use of LSL is considered vital for the synchronous recording of data, other designs may satisfy the same principle. Instances of such designs could be the direct streaming of the data to a python interface, whereby the synchronization could take place hand in hand with the data analysis (in such case, we would have steps 1, 3, and 4 of **Figure 3** of the main text**,** step 2 would not be needed).

Other possible variations are that someone could create different experimental concepts and procedures, applied to different populations, or use different devices and methods to create sensory augmentation/substitution.

Sensory Feedback Augmentation

Numerous variations could be applied on the way that sensory-feedback augmentation is created. In the interface example 1 (see section "EXAMPLE 1, Supplementary File), we take the inter-peak-interval (IPI) times of the heartbeats and use their length to define the speed of the played song. This process is happening in real-time and the updates of the song are taking place continuously during the experiment. As a result, the song is changing speed constantly.

Alternatively, we could extract audio features from the MMS trains or the original signal, using the MATLAB MIR toolbox or other methods, and use them to alter different features of the sound.

Likewise, with the visual feedback (*e.g.* provided by the avatar, see section "Example 2", Supplementary File) we can alter the real-time motions that we endow the avatar with, using noise portrays extracted from databanks of motion data collected from the person. We can also endow the avatar with the veridical motions from the user, while delaying them to test the person's limits in gaining awareness of the delays. We can manipulate other properties such as color, brightness, and contrast of the 3D rendering, and as in this example, add audio to enhance the visuo-motor experience.

Other sensory modalities could be used as a means of feedback in similar interfaces. Modern technology allows us to generate sensations such as haptic, olfactory, to name a few, which could be incorporated in a co-adaptive interface

EXAMPLE 1: AUDIO CLOSE-LOOP INTERFACE OF A REAL DYADIC INTERACTION

Two salsa dancers performed a well-rehearsed routine staging a choreography and a spontaneously improvised dance. The dancers had to perform the original version of the song and a version blended with the real-time speed of the heartbeat stream.

The proxy control interface used to blend the speed of the heartbeat with the speed of the song is illustrated in **Figure 4** of the main text. We used the female dancer's heart signals to extract the heartbeat times and alter the music. In real time, we performed signal processing of the ECG signal to extract the times of the R peaks and estimate their IBI timings. Then, we streamed this information to MAX where it defined the speed of the played song. This way, the played song was altered by the biophysical signals. This process led to further alterations of the motions and heartbeat signals, which we were continuously re-parameterizing.

Participants

Two experienced salsa dancers (a male and a female, 30 years old) participated in the experiment which was approved by the Rutgers University Institutional Review Board in accordance with the Helsinki Act.

Set-up of the Audio Close-loop Interface

Set-up kinematic and EEG equipment -ANS, PNS, and CNS

A 32-channel EEG system was used to record brain activity as well as the HR of the female dancer. Twelve inertial measurement units (IMU) were also used to record bodily activity. The latter signals are used offline and currently are not part of our online streaming and analyses described in our interface. Their analysis is presented in [1].

To prepare the EEG system, follow the steps presented in sections 2.2 and 2.3 of "Set-up of the Close-Loop Interface" of the main text.

Preparation and set-up of LSL for synchronized data recording and streaming of data

For the synchronous recording of the data in LSL, we followed the step presented in sections 2.5 and 2.6 of "Set-up of the Close-Loop Interface" of the main text.

The real-time analyses of data and monitoring of the human system

A Python interface is designed to continuously receive chunks of data streamed by the LSL at a frequency of 500Hz. Once the interface receives the first chunk, it sends a signal to start the Max interface. At the beginning of the recording, the interface buffers 2000-frame-long data (equal to 4sec, enough to detect R-peaks of the ECG signal), which is utilized as an assistive vector. Once it collects those frames, it starts processing the data to detect peaks and stream those to Max.

Specifically, on each frame, the system adds the new value to the end of the buffer and dismisses the oldest value. The updated buffer with the ECG data is filtered using the Butterworth IIR band pass filter for 5-30Hz at 2nd order. The range of the band pass filter is selected based on the finding that a QRS complex is present in the frequency range of 5-30Hz. Then, we use the *peakutils.indexes Python* function (threshold is set 0.7 and minimum distance is equal to 110) to detect the R peaks' amplitude values and their times of occurrence. Each time the interface detects a new peak in the buffer, it sends 1 to Max, otherwise it sends 0.

To achieve the closest to real-time streaming, we designed our algorithm to stream 1 when detecting a peak at the most recently added frame, the last one, while accounting for the time it takes to filter and process these values. Such time periods are variable because they require forecasting the future trend of the signal. As a result, we had to detect peaks at a consistently earlier frame and estimate forward. To that end, we empirically examined different values of n number of earlier frames and investigated the limiting cases, so that n had the smallest possible value (be as recent as possible) and the corresponding ECG value had enough neighbour values to be filtered and be processed properly for reliable forward estimation. Initial stages to build the interface took extensive experimentation, upon which we settled on n = 10. Clearly, this choice will depend on sampling resolution and needs to be individualized. In the present examples, this value provides good buffering while delaying 1/50 sec. Future work will involve researching other methods of time series forecasting and quick detection methods, to optimize the buffering-window size. The interface can also save the raw data collected during a session for later analysis. These data were used to aid calibrate the buffering time in a personalized manner.

Finally, once the recording is complete the interface sends a signal to stop the Max interface.

The code that performs this analysis can be found at https://github.com/VilelminiKala/CloseLoopInterfaceJOVE.

Generation of the sensory feedback

The peaks detected by the Python interface are sent to the playback interface. Specifically, we

sent 1 each frame a heartbeat is detected, and we sent 0 otherwise. This is done with software designed using the musical programming language (cycling74.com). Filtered heart R peaks are transmitted in real time to Max from the Python script via Open Sound Control (OSC) (http://opensoundcontrol.org/). Additionally, signals to start and stop playback, as well as an index value of peak numbers used for testing the system are also transmitted to Max via OSC. Within the playback interface, the inter-peak intervals are measured and converted to beats per minute. This data is scaled to create a playback speed scaling factor between 0 (slowest possible playback) and maximum playback speed (fastest possible playback). On this continuum, 1 equals "normal" playback speed, 0.5 equals half speed, and 2 equals double playback speed. There are two modes for data scaling, a positive correlation linear scale, where an increase in the dancers' heart rate will produce faster playback, and a negative correlation linear scale, where an increase in the dancers' heart rate will produce slower playback. The playback speed scaling factor is continuously adjusted in real time based on the incoming heart rate data. **Supplementary Table 1** shows how the duration of the songs varies from repetition to repetition. Using Max's sfplay~ object, any audio file may be loaded into the software. Playback is controlled in one of two modes: playback speed, where slower playback speed produces a lower pitch, as in the playback of analog recordings, or time-stretch mode, where playback speed and pitch are decoupled. The latter is what was used in the current experimental procedure.

[Place supplementary Table 1 here]

Experimental Procedure

The task consisted of two parts. Part 1 was to perform a well-rehearsed routine staging a choreography. Part 2 was to spontaneously improvise. The dancers had to perform each song at each original version (baseline) and then do so two more consecutive times, while the song was blended with the real-time speed of the heartbeat stream.

The design of this experiment was extended to works [1-5]

EXAMPLE 2: AUDIO-VISUAL CLOSE-LOOP INTERFACE OF AN ARTIFICIAL DYADIC INTERACTION

The participant faces a large screen monitor and sees the 3D rendered image of the moving avatar (as in **Figure 2B** of the main text) endowed with the real-time movements' output registered by the motion-capture system using active LEDS. As the person moves mirroring the avatar, we manipulate the environment by embedding position-dependent sounds within the region surrounding the person. The person is not aware of these sound-triggering positions, denoted regions of interest, RoI. We define such RoIs across the space where the person moves. As some body part (e.g. the hip) passes through a RoI, the computer program toggles music play. If the person sustains the pose with the body part in that RoI, the computer program continuous playing the music, but if the person moves the body part away from the RoI, then the music stops playing. This can turn the search for RoIs denoting musical spots into a game across space. The idea is to raise awareness about several aspects of actions and environmental cues that we automatically process beneath awareness.

To further play with the person's ability to build maps between body poses and musical bits, we also may anchor the RoI to a specific body part and play the music faster or louder, etc. as a function of the person's movement. For example, we can play the music faster or slower, depending on how close or far the hand is by the center of the RoI. Once the person finds the RoI, we can shift its location in space and define a new RoI to gamify the session and evoke curiosity. Importantly the person is naïve to these experimental goals and has to figure them out by self-discovering what the goals are (as autistic children did in [6]).

Participants

Six young adults participated in this experiment. They signed the consent form approved by the IRB of Rutgers University, in compliance with the Helsinki act.

Set-up Audio-Visual Close-Loop Interface

Set-up kinematic and EEG equipment -ANS, PNS, and CNS

A motion-capture system was used to record bodily positions using an LED based motion-tracking system. The EEG was used to record the brain activity and heart signal. To prepare the equipment, we followed all the steps presented in sections 2.1, 2.2, and 2.3 of "Set-up of the Close-loop Interface" of the main text.

Preparation and set-up of LSL for synchronized data recording and streaming of data

For the synchronous recording of the data in LSL, we followed the steps presented in section 2.4, 2.5, and 2.6 of "Set-up of the Close-Loop Interface" of the main text.

The real-time analyses of data and monitoring of the human system

We developed our methods to parameterize the fluctuations in the efferent motor output

Visual 3D representation of the human body

To represent the human body in 3D, we developed an avatar using MATLAB graphics. To that end, we obtained the positions of 23-body-part skeleton streamed from motion-capture system (**Figure 8** step 2 of the main text) to LSL and then from LSL to MATLAB (**Figure 8** step 3 of the main text). The position data of the skeleton coming in chunks were used to estimate the rotations between the body-parts and build a forward kinematic map. The full-body forward kinematic map was developed based on the arm model described in [7]. Using the hip as the origin of the reference frame to build the skeleton (bone 0, **Figure 8** step 3 of the main text), we developed 5 kinematic chains spine-head, right arm, left arm, right leg, left leg. The left and right arms were initiated by the bone 2 (**Figure 8** step 3 and 4 of the main text), whereas the rest of the chains were initiated by the hips (bone 0, **Figure 8** step 3 of the main text).

To estimate the positions of the rigid bodies in MATLAB, we set the position of the origin rigid body equal to the position of bone 0, at the hips. Thus, $RB_o=B_0$, where RB_n is the position of rigid body part n and B_n is the position of bone n as it is originally streamed from LSL. To

estimate the positions of the rest of the rigid bodies we used Equation (2).

$$RB_{n+1} = RB_n + (Rot_0 * \cdots * Rot_{n+1}) * [0, 0.BL_{n+1}] \quad (2)$$

where BL_n in the 3x1 vector is the bone length of bone n and the 3x3 matrix Rot_n is the rotation matrix of bone n. Equation (2) is the generalized model of the forward-kinematic map presented in [7] which was designed to model human arm motions only. We here extend the previous work to a full-body model. In the arm model the kinematic chain starts from shoulder, whereas our full body version has 5 kinematic chains, three of which start from the hips, bone 0, and 2 start from the bone 2. Shown in **Figure 8** step 4 (of the main text) after the kinematic chain of spine-head is estimated.

We developed the forward kinematic map of the Avatar in MATLAB (version 2016b, The MathWorks, Inc., Natick MA, USA.). The code can be found here: https://github.com/VilelminiKala/CloseLoopInterfaceJOVE

Audio parameterization

The parameterization of the audio feedback was different across conditions. These are listed in **Supplementary Figure 1**.

[Place supplementary Figure 1 here]

In the 1st condition, the sound was activated when the participant walked through a specific area defined by the proxy controller. The 3D center position of this area was entered by the researcher by clicking the proper button on the proxy controller (user interface) during the recording setting. The instant position of the hips of the moving participant was then set as the center of the song-activation body part. The system could also use other body parts as the anchor to manipulate the music. The researchers could also manually set the radius of that RoI before starting the recording to define a volume between the desired position and the position of the body part. In our example, the radius was set to 50cm. As the participant found and maintained their position within the RoI, the song would play for as long as the participant stayed within that volume.

In the 2nd condition, the hips once again controlled the activation of the song, but the sampling rate of the song's playback was defined by the distance between the center of the activation area and the hand. Specifically, we created a grid of zones using distances at every 10cm. In the case of radius = 50cm, there were 5 zones of distance. The min sampling rate was set to a minimum of 95 frames per second and the maximum sampling rate was set to the original sampling rate. The interface could create a grid of n zones around the hip, 5 in our example, based on hand-to-activation-point distance of each person, and accordingly, modulate the sampling rate of the music playback.

In the 3rd condition, the speed of the participant's hips, was used to control the sampling rate of the song. In this condition, the interface created 5 zones of sampling rate ranging from a minimum of 1000 frames per second to the maximum set as the original sampling rate. The

sampling rate was set to minimum when speed was smaller than V_{min} value and to maximum when speed was greater than V_{max}. To define these two parameters, the speed ranges of the hip of each participant were previously recorded and extracted from their walking pattern. Thus, V_{min} and V_{max} was chosen (by the researchers) to belong in the individuals speed range but also based on how sensitive or stable the system should be, depending on its use. The completion of each task was defined by the participant's self-discovery of the interaction rules, while maintaining their speed steady, to be able to listen to the song. We underscore that the participants were naïve to what they needed to self-discover.

Generation of the Sensory Feedback

Visual Feedback

The proxy controller generates a real-time 3D representation of the participant, an avatar, which is used as a mirror, with the purpose of enhancing the person's kinesthetic feedback and self-awareness. **Supplementary Figure 1** shows the setup of the visually driven proxy control.

The MATLAB code (version 2016b, The MathWorks, Inc., Natick MA, USA.) that uses the presented forwards kinematic map and generates the avatar presented in **Supplementary Figure 1** and **Figure 8** of the main text can be located in https://github.com/VilelminiKala/CloseLoopInterfaceJOVE

Audio Feedback

The music was played back through the Matlab interface (Matlab version 2016b, The MathWorks, Inc., Natick MA, USA.). The MATLAB function used for playing the song was: *audioplayer(Y, Fs)*, where Y is the time series song signal and Fs is the sampling frequency.

Experimental Procedure

The participants were naïve as to the purpose of the study. They had to walk around the room and figure out how to control the sound that would surprisingly emerge as they passed by a RoI that the proxy controller defined.

In condition 1, the position of the hips controls the activation of the music. As the participant's hips entered a RoI that the proxy controller defined, the music played. The music playing occurred as a direct consequence of the person's action (i.e. moving into the RoI). Since this action's consequence surprised the participant, she initiated the search for the "magic" position that played music (i.e. the antecedent to the consequence.) During this exploratory motion, the activity corresponding to the search in the space outside the RoI was processed and compared to the activity harnessed while being inside the RoI. The exploratory *vs.* target activity bear different contextual signatures of motor-based feedback. As such, it was important to characterize them for each person.

In condition 2, the position of the hips controls the activation of the music, as in condition 1, but now the distance of the right hand from the center of the hip-anchored RoI served to set the control of the sampling rate to play the song back faster or slower.

In condition 3, the walking speed at the hips was used to control the sampling rate of the music playback: faster speed led to faster song playback.

The design of the interface was developed as part of the first author's PhD Thesis [2], and it is also presented also in [3,8]. It stems from US patented technology found at https://patents.google.com/patent/US10176299B2/en?inventor=Elizabeth+B.+TORRES, which was initially applied to new sensory-motor based interventions for autism [6].

DATA TYPES AND ANALYSES

In our representative examples, the signal analyses (the results of which are presented in section "Representative Results" of the main text) consist of two main steps: first we create a data type called the micro-movement spikes (MMS trains) and second, we use the spikes as input to a Gamma process. We use this process to update the stochastic signatures denoting the evolution of the noise-to-signal ratio and track the changes in the shape and the scale of the empirically defined family of continuous probability distribution functions (PDFs).

Micro-movement Spikes

The MMS are derived from the fluctuations in the amplitude of the peaks of the time series signal. They can also be derived from the fluctuations in the inter-peak interval times. In this work, we use the MMS trains derived from the fluctuations in both amplitude and timing related signals. For example, the raw peak amplitude is normalized using equation (1) [9]:

$$Normalized\ Peak\ Amplitude = \frac{Peak\ Amplitude}{Peak\ Amplitude + Average_{Min\ to\ Min}} \quad (1)$$

Here the Peak refers to the amplitude of the local peak and min to min refers to the two neighboring minima surrounding the local peak. All points sampled between these local minima (including the local peak) are averaged and added to the local peak, to build the denominator term. Importantly, the fluctuations are computed relative to the empirically derived overall mean of each window of data (under independent identically distributed iid assumption.)

The MMS, which are real numbers ranging in the [0,1] real interval maintain the information of the peak timing and/or amplitude. At the same time, they enable us to treat the time series as a random process. We use a Gamma process under the general rubric of Poisson random processes. Poisson-based analyses are commonly used in the field of computational neuroscience aiming to analyze binary spikes (*e.g.* from cortical signals.) We have adapted this approach to study continuous MMS trains derived from peripheral signals [10-14]

Gamma Distribution

A random variable X that is Gamma distributed with shape a and scale b is denoted by $X \sim \Gamma(a,b) = Gamma(a,b)$ with probability density function:

$$F(x,a,b) = \frac{x^{a-1} * e^{-x/b}}{b^a \Gamma(a)}, \text{ for } x > 0 \text{ and } a, > 0 \qquad (3)$$

Here x is the random variable of interest and Γ is the Gamma function. The Gamma mean $\mu = a*b$ and the variance $\sigma = a * b^2$ with the noise to signal ratio given by equation (4)

$NSR = \sigma/\mu = b$ (4)

The NSR is thus the scale parameter in the continuous Gamma family. In this work, we use the continuous data stream of normalized peak values derived from the fluctuations in the heart signal amplitude and the music to estimate the Gamma mean for each block of data buffered (as explained above) and to obtain the Gamma moments.

We track the shape and scale parameters empirically estimated each time step, using MLE with 95% confidence intervals.

Maximum Likelihood Estimation for each condition shows best fitting for the continuous Gamma distribution with maximum value at 0 gradient convergence, see **Supplementary Figure 2**. Frequency histograms of the MMS are shown as insets with fitted distributions using the MATLAB distribution fitting app.

[Place supplementary Figure 2 here]

Stochastic Analyses

These methods have been explained in previous work[4,8,10,11,13-18] We define the Gamma parameter plane with axes described by the shape and scale parameters of the Gamma probability density functions (PDFs) that we empirically estimate using the MMS (see **Figure 9** of the main text). We also plot the corresponding Gamma moments because in our experience, they offer good visualization and automatic clustering of various populations and/or contexts, parameters, etc. Specifically, on a four-dimensional graph, we plot the mean, variance and skewness along the X, Y, Z dimensions respectively (see **Figure 6C** of the main text). We represent the point by a marker and scale the size of the marker proportional to the kurtosis, as the fourth dimension. We may also color the marker's face and edge using raw data ranges and derive other indexes to represent the phenomena in more compact formats using other parameter spaces.

For each case, the MMS trains are gathered in a frequency histogram. Then empirical distribution fitting is performed using maximum likelihood estimation (MLE) with 95% confidence intervals. We estimate the best continuous family of PDFs for the data at hand. In MMS derived from human biorhythms, the continuous Gamma family of PDFs has been adequate to fit these frequency histograms, see **Supplementary Figure 2 and 3**. Then we represent the Gamma parameters in a parameter plane: the shape denoting the distribution's shape, and the scale denoting the dispersion (noise to signal ratio), see **Supplementary Figure 3**.

This empirical estimation captures the signatures of biorhythmic fluctuations of the person's nervous systems for each of the signals that each of the instruments registers. This approach contrasts with traditional methods assuming *a priori* some theoretical distribution. In human data, it has been our experience that a log-log transform of the data aligns the points along a line of unity across multiple decades of the shape parameter values (a power law) with tight fit. In such cases, we reduce the parameters of interest to one (the noise to signal ratio, or Gamma scale) since, knowing the noise, we can safely infer the shape of the distribution [19,20]. These estimations are performed for each context and condition and tracked in real time across the experimental session. **Supplementary Figure 3** shows the pipeline of these analyses using traces from the hip's motions as an example. We have characterized across disorders of the nervous systems the healthy regimes of noise and identified phase transitions denoting learning and adaptation regimes differentiating novice- from expert-like signatures (see **Supplementary Figure 3F** and [19]).

[Place supplementary Figure 3 here]

FIGURES AND TABLES

Supplementary Table 1: The duration of the original and the altered songs. The speed of the altered songs is continuously updated during the experiment based on the ongoing speed of the heartbeat. Therefore, none of the altered recording matches neither with the original song nor with other altered versions of the same song

Supplementary Figure 1: Conditions of the audio-visual interface. In the first condition, the position of hips activates the music when they are in a spherical RoI (radius 50cm around the hip which is set as the origin). In the second condition, the position of hips activates the music as in condition 1 and the distance of the right hand from the center of the RoI defines the sampling rate that plays the song. In the third condition, the speed of the hips walking around the room sets the sampling rate of the song playback.

Supplementary Figure 3: Standardized MMS data type and analytical pipeline. (A) Sample 3D trajectory from a light emitting diode (LED) located on one of the hips, harnessing motion as the person dances to music. Red dots indicate the peaks of the linear speed. (B) Linear speed profiles with peaks signaling maxima, change in slope (positive to negative) as the body moves (accelerates and decelerates) for 166.66 seconds (2.77 minutes, sampling at 480Hz with the motion-capture system active LED-camera system). (C) Micro-movement spikes (normalized peaks extracted from the linear speed, marked in red in (B) using equation (1) and obtaining the absolute deviations from the mean amplitude. Full MMS trains including all peaks and pauses of the 4.5×10^4 frames. (D) Frequency histograms of the raw (cm/frame) and normalized (unitless) MMS. The bin size of the histograms is defined by the Scott's rule. (E) Best fitting Gamma PDFs using MLE and 95% confidence intervals to estimate the shape and scale parameters and the corresponding histograms of two extreme cases. The bin size of the graphs has been estimated by Scott's rule (F) Gamma parameter plane showing the three corresponding (shape, scale) points

and their empirical determined interpretation along the color scale.

REFERENCES

1 Kalampratsidou, V. & Torres, E. B. Sonification of heart rate variability can entrain bodies in motion. *Proceedings of the 7th International Conference on Movement and Computing.* 10.1145/3401956.3404186 Article 2, (2020).

2 Kalampratsidou, V. *Co-adaptive multimodal interface guided by real-time multisensory stochastic feedback*, Rutgers University-School of Graduate Studies, (2018).

3 Kalampratsidou, V., Kemper, S. & Torres, B., Elizabeth. Real time streaming and closed loop co-adaptive interface to steer multi-layered nervous systems performance. *48th Annual Meeting of Society for Neuroscience.* (2018).

4 Kalampratsidou, V. & Torres, E. B. Bodily Signals Entrainment in the Presence of Music. *Proceedings of the 6th International Conference on Movement and Computing.* 3, (2019).

5 Kalampratsidou, V., Zavorskas, M., Albano, J., Kemper, S. & Torres, E. B. Dance from the heart: A dance performance of sounds led by the dancer's heart. *Sixth International Symposium on Movement and Computing.* (2019).

6 Torres, E. B., Yanovich, P. & Metaxas, D. N. Give spontaneity and self-discovery a chance in ASD: spontaneous peripheral limb variability as a proxy to evoke centrally driven intentional acts. *Frontiers in integrative neuroscience.* **7** 46, (2013).

7 Torres, E. B. *Theoretical Framework for the Study of Sensori-motor Integration.*, University of California, San Diego, (2001).

8 Kalampratsidou, V. & Torres, E. B. Body-brain-avatar interface: a tool to study sensory-motor integration and neuroplasticity. *Fourth International Symposium on Movement and Computing, MOCO.* **17**, (2017).

9 Lleonart, J., Salat, J. & Torres, G. J. Removing allometric effects of body size in morphological analysis. *J Theor Biol.* **205** (1), 85-93, (2000).

10 Torres, E. B., Vero, J. & Rai, R. Statistical Platform for Individualized Behavioral Analyses Using Biophysical Micro-Movement Spikes. *Sensors (Basel).* **18** (4), (2018).

11 Torres, E. B. & Denisova, K. Motor noise is rich signal in autism research and pharmacological treatments. *Scientific Reports.* **6** 37422, (2016).

12 Torres, E. B. Two classes of movements in motor control. *Experimental Brain Research.* **215** (3-4), 269-283, (2011).

13 Torres, E. B. *et al.* Characterization of the statistical signatures of micro-movements underlying natural gait patterns in children with Phelan McDermid syndrome: towards precision-phenotyping of behavior in ASD. *Frontiers in integrative neuroscience.* **10** 22, (2016).

14 Wu, D. *et al.* in *APS March Meeting Abstracts.*

15 Torres, E. B. *Objective Biometric Methods for the Diagnosis and Treatment of Nervous System Disorders*. (Academic Press, Elsevier, 2018).

16 Torres, E. B. *et al.* Toward Precision Psychiatry: Statistical Platform for the Personalized Characterization of Natural Behaviors. *Frontiers in neurology.* **7** 8, (2016).

17 Kalampratsidou, V. & Torres, E. B. Outcome measures of deliberate and spontaneous

motions. *Proceedings of the 3rd International Symposium on Movement and Computing.* 9, (2016).

18 Kalabratsidou, V. & Torres, E. B. Invariant and variable relations emerge with degrees of difficulty within habitual and surprise touch-pointing motions. *Journal of Vision.* **14** (10), 418-418, (2014).

19 Torres, E. B. Signatures of movement variability anticipate hand speed according to levels of intent. *Behavioral and Brain Functions.* **9** 10, (2013).

20 Torres, E. B. *et al.* Autism: the micro-movement perspective. *Frontiers in integrative neuroscience.* **7** 32, (2013).